

# Strong angular momentum optomechanical coupling for macroscopic quantum control

Yuan Liu,<sup>1,2</sup> Yaoming Chu,<sup>1,2</sup> Shaoliang Zhang,<sup>1,2,\*</sup> and Jianming Cai<sup>1,2,†</sup>

<sup>1</sup>*School of Physics, Hubei Key Laboratory of Gravitation and Quantum Physics, Institute for Quantum Science and Engineering, International Joint Laboratory on Quantum Sensing and Quantum Metrology, Huazhong University of Science and Technology, Wuhan 430074, China*

<sup>2</sup>*Wuhan National Laboratory for Optoelectronics, Huazhong University of Science and Technology, Wuhan 430074, China*  
(Dated: March 8, 2024)

Optomechanical systems offer unique opportunities to explore macroscopic quantum state and related fundamental problems in quantum mechanics. Here, we propose a quantum optomechanical system involving exchange interaction between spin angular momentum of light and a torsional oscillator. We demonstrate that this system allows coherent control of the torsional quantum state of a torsional oscillator on the single photon level, which facilitates efficient cooling and squeezing of the torsional oscillator. Furthermore, the torsional oscillator with a macroscopic length scale can be prepared in Schrödinger cat-like state. Our work provides a platform to verify the validity of quantum mechanics in macroscopic systems on the micrometer and even centimeter scale.

**Introduction.**— Optomechanics is currently under intense research focus [1–9], aiming for coherent manipulation of the quantum states of macroscopic objects [1–6]. As an versatile platform to investigate fundamental problems in quantum mechanics, quantum optomechanics provides a route towards generation of macroscopic quantum states [6–11]. It is remarkable that macroscopic quantum states, such as Schrödinger cat states [12] (namely coherent superposition of two macroscopically distinct states), phonon addition and subtraction states [10, 11], are of great significance in exploring the boundary of quantum theory [13] and the validity of collapse models [14].

In most optomechanical systems, the optomechanical interaction between light and matter is induced by the linear momentum exchange interaction. However, the angular momentum of light can also be utilized to contribute the exchange interaction between light and matter [15–19]. This opens the door to new possibilities in the engineering of optomechanical system. For example, the angular momentum of light may provide an effective way to manipulate the rotational quantum state of a spiral phase plate [20], and to drive the rotational degree of other mechanical oscillators, such as levitated nanoparticles [21–23] and integrated optical waveguides [24, 25]. Despite these exciting developments, the challenge remains in achieving strong angular momentum optomechanical interaction between light and torsional oscillators with macroscopic length scale [21–25], which would lead to interesting macroscopic quantum phenomena and extend the research scope of quantum optomechanics.

In this Letter, we theoretically propose an optomechanical system with strong exchange interaction between spin angular momentum of light and a long (length  $L \approx 0.1\text{mm} - 1\text{cm}$ ) torsional oscillator of optical anisotropy and demonstrate the effectively cooling, squeezing and Schrödinger catlike state [26] preparation of the torsional degree of freedom of the torsional oscillator. The torsional motion of the optical anisotropic torsional oscillator induces cross optomechanical coupling between two orthogonal optical modes and the torsional motion mode. With feasible experimental parameters, the optomechanical coupling strength can reach the order of 20kHz, which

can be further amplified into the strong coupling regime [27] (i.e. optomechanical coupling coefficient  $\chi \geq 1$ ) by using a coherent laser to pump one of the orthogonal polarization mode. This enables us to control the torsional quantum state of the torsional oscillator using only a few photons of the other optical mode, even though the original optomechanical coupling strength does not satisfy the usual single-photon strong coupling condition [28]. Based on this system, it is feasible to prepare the torsional oscillator into a coherent superposition state of two macroscopically distinct torsional quantum states, thus provides a platform to explore the fundamental problems related with quantum torsional motion, such as the macroscopic decoherence, rotational friction and diffusion of a long quantum torsional oscillator [29, 30]. Therefore, our system greatly enriches the toolbox of quantum optomechanics.

**The model.**—The optomechanical resonator that we consider is a suspended square beam [31–33] with length  $L$  and width  $a$  ( $L \gg a$ ), the basic structure of which is presented in Fig. 1. The optical anisotropy of this optomechanical resonator results in the following relative permittivity tensor  $\epsilon$

$$\epsilon = \begin{pmatrix} \epsilon_{xx} & 0 & 0 \\ 0 & \epsilon_{yy} & 0 \\ 0 & 0 & \epsilon_{zz} \end{pmatrix}, \quad (1)$$

where  $\epsilon_{ii}$  is the relative permittivity in the  $i$  ( $i = x, y, z$ ) direction in laboratory frame. This optomechanical resonator supports two fundamental orthogonal quasi-linear polarization optical modes [34] with the corresponding electric field profiles  $\mathbf{E}_1(\mathbf{x}) = \mathbf{E}_1(x, y) \cos(\beta_1 z) \exp(i\omega_1 t)$  and  $\mathbf{E}_2(\mathbf{x}) = \mathbf{E}_2(x, y) \cos(\beta_2 z) \exp(i\omega_2 t)$  [35, 36], where  $\beta_1$  and  $\beta_2$  are the propagation constants of  $\mathbf{E}_1(\mathbf{x})$  and  $\mathbf{E}_2(\mathbf{x})$ , respectively. The total electric field operator can be written as  $\mathbf{E}(\mathbf{x}) = \mathbf{E}_1(\mathbf{x})a_1 + \mathbf{E}_2(\mathbf{x})a_2 + h.c.$ , where  $a_1$  and  $a_2$  are the annihilation operators of two optical modes, which satisfy bosonic commutation relation  $[a_i, a_j^\dagger] = \delta_{ij}$  ( $i, j = 1, 2$ ).

From a mechanical point of view, the torsional wave in a mechanical oscillator with  $L \gg a$  can be described by one-

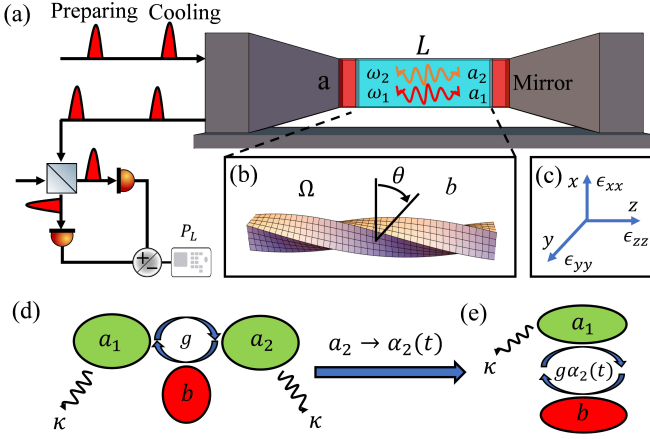


Figure 1. (a) Sketch showing the experimental embodiment of this optomechanical resonator. The length of optomechanical resonator is  $L$  and the width is  $a$ . The frequency of mechanical mode  $b$  is  $\Omega$  and the frequencies of the optical modes  $a_1$  and  $a_2$  are  $\omega_1$  and  $\omega_2$ , respectively. (b) The torsional mode of the optomechanical resonator with the relative permittivity  $\epsilon_{ii}$  (c) in the  $i$  ( $i = x, y, z$ ) direction. (d) The optomechanical resonator couples with the two optical modes, the optomechanical coupling strength of which is denoted as  $g$ , see Eq.(5). (e) shows the effective coupling between the torsional mode  $b$  and the optical mode  $a_1$  when the optical mode  $a_2$  is classically driven by a coherent laser pulse with the characteristic parameter  $\alpha_2(t)$ .

dimensional Webster-type wave equation [37, 38]

$$c_t^{-2} \partial_t^2 \phi(z, t) - \partial_z^2 \phi(z, t) - \left( \frac{\partial_z I_p(z)}{I_p(z)} \right) \partial_z \phi(z, t) = 0, \quad (2)$$

where  $I_p(z) = \int_A r^2 dA$  is the polar moment of inertia at the cross section  $A(z)$ ,  $c_t$  is the phase velocity of torsional wave,  $\phi(z, t) = \theta(z) \cos(\Omega t)$  is the amplitude of angular displacement with  $\Omega$  the torsional resonance frequency and  $\theta(z)$  the spatial mode function of torsional motion. In order to decrease mechanical dissipation [37, 39], we will focus on the fundamental mode of torsional motion which can be supposed as  $\theta(z) \propto \cos(k_t z)$  [34, 39] where  $k_t = \Omega/c_t$ . By introducing phonon annihilation operator  $b$  and creation operator  $b^\dagger$ , we can express the Hamiltonian of the torsional motion as  $H_m = \hbar\Omega(b^\dagger b + 1/2)$  [39]. The zero point angular displacement is given by  $\theta_{zp} = \sqrt{\hbar/(2I_{\text{eff}}\Omega)}$ , where  $I_{\text{eff}}$  is the effective moment of inertia.

The Hamiltonian of electromagnetic field can be written as  $H_{\text{em}} = 1/2 \int_V dV (\epsilon_0 \mathbf{E}(\mathbf{x}) \cdot \epsilon(\mathbf{x}) \mathbf{E}(\mathbf{x}) + \mu_0 \mathbf{H}(\mathbf{x}) \cdot \mu(\mathbf{x}) \mathbf{H}(\mathbf{x}))$  [40]. The torsional motion of the optomechanical resonator will influence the relative permittivity  $\epsilon$ , and thus affect the Hamiltonian  $H_{\text{em}}$ . If we neglect opto-elastic effect [41, 42] and moving boundary effect [42, 43], the relative permittivity  $\epsilon(\theta)$  of the torsional motion can be estimated as [34]

$$\epsilon(\theta) = R(\theta)\epsilon(0)R(-\theta) \quad (3)$$

where  $\epsilon(0) = \epsilon$  and  $R(\theta) = \begin{pmatrix} \cos(\theta) & -\sin(\theta) & 0 \\ \sin(\theta) & \cos(\theta) & 0 \\ 0 & 0 & 1 \end{pmatrix}$  is a

rotation matrix. Expanding  $R(\theta)$  to the first order of  $\theta$ , we can derive the approximated expression of  $\epsilon(\theta)$  as

$$\epsilon(\theta) = \epsilon(0) + \delta\epsilon\theta(z)A \quad (4)$$

where  $\delta\epsilon = \epsilon_{xx} - \epsilon_{yy}$  and  $A = \begin{pmatrix} 0 & 1 & 0 \\ 1 & 0 & 0 \\ 0 & 0 & 0 \end{pmatrix}$ . The matrix

$A$  mixes two optical modes  $a_1$  and  $a_2$  in Hamiltonian  $H_{\text{em}}$  and induces exchange interaction between the optical modes  $a_1$  and  $a_2$ . Finally, we can obtain the total optomechanical Hamiltonian as

$$H_{\text{OM}} = \hbar\Omega b^\dagger b + \hbar\omega_1 a_1^\dagger a_1 + \hbar\omega_2 a_2^\dagger a_2 + \hbar g(b + b^\dagger)a_1^\dagger a_2 + \hbar g^*(b + b^\dagger)a_2^\dagger a_1 \quad (5)$$

where  $g$  is the optomechanical coupling strength. We note that the effective Hamiltonian of the similar form can also be found in coupled-cavity optomechanical systems [44–46] with promising applications powered by the single-photon non-linearities optomechanical interaction [46] and enhanced quantum non-linearities optomechanical interaction [44].

The coupling strength plays a vital role in quantum optomechanics. In the present system,  $g$  can be estimated as [34]

$$g \propto \theta_{zp} \sqrt{\omega_1 \omega_2} \left( \frac{\delta\epsilon}{L} \right) \int_{-L/2}^{L/2} \theta(z) \cos(\beta_1 z) \cos(\beta_2 z) dz. \quad (6)$$

The coupling strength  $g$  is proportional to the optical anisotropy  $\delta\epsilon$  of the torsional oscillator, see Eq.(4). The integral factor in Eq.(6) is determined by the wave vectors  $\beta_1$  and  $\beta_2$  of the two optical modes and the wave vector  $k_t$  of the torsional mode. We remark that the other optomechanical coupling mechanisms which are widely involved in integrated optomechanical systems [10, 47, 48], such as moving boundary coupling effect [42, 43] and opto-elastic coupling effect [41, 42], will also contribute to  $g$ . Nevertheless, our analysis detailed in Supplementary Material [34] shows that for the torsional motion considered in our system, the contributions of these effects are much less significant than the contribution of the optical anisotropy and can be neglected in the present system.

*Single-photon optomechanical coupling.*— To achieve strong optomechanical coupling at the single-photon level, we set two optical modes  $a_1$  and  $a_2$  as degenerate with  $\omega_1 = \omega_2$  [49]. Then the Hamiltonian  $H_{\text{OM}}$  in Eq.(5) can be expressed in interaction picture as  $H_{\text{OM}} = \hbar g (b e^{-i\Omega t} + b^\dagger e^{i\Omega t}) (a_1^\dagger a_2 + a_2^\dagger a_1)$ . Using a strong coherent laser to pump the optical mode  $a_2$ , the intracavity operator  $a_2$  can be treated classically and the Hamiltonian  $H_{\text{OM}}$  becomes

$$H_{\text{OM}}^{\text{new}} = \hbar g \alpha_2(t) (b e^{-i\Omega t} + b^\dagger e^{i\Omega t}) (a_1^\dagger + a_1), \quad (7)$$

where  $\alpha_2 = \langle a_2 \rangle$ ,  $\int |\alpha_2(t)|^2 dt \approx 4N_{\text{in}}/\kappa$  [34],  $N_{\text{in}}$  is the total input photon number of a single coherent pulse and  $\kappa$  is the decay rate of the cavity. Without loss of generality, we assume that  $\alpha_2$  is a real number. By defining

Table I. Parameters of the optomechanical system

$\lambda/\text{nm}$	$Q_o$	$\kappa/\text{MHz}$	$\tau^{-1}/\text{MHz}$	$\Omega/\text{kHz}$	$Q_m$	$I_{\text{eff}}/\text{kg} \cdot \text{m}^2$	$\theta_{zp}$	$g/\text{kHz}$
1550	$8.4 \times 10^5$	$2\pi \times 225$	$2\pi \times 15$	$2\pi \times 500$	$1 \times 10^4$	$4.4 \times 10^{-25}$	$6.16 \times 10^{-9}$	22

$\hat{x}_L = (a_1^\dagger + a_1)/\sqrt{2}$ ,  $\hat{p}_L = i(a_1^\dagger - a_1)/\sqrt{2}$ ,  $\hat{\theta}_M = (b^\dagger + b)/\sqrt{2}$ ,  $\hat{L}_M = i(b^\dagger - b)/\sqrt{2}$ , the Hamiltonian  $H_{\text{OM}}^{\text{new}}$  becomes  $H_{\text{OM}}^{\text{new}} = 2\hbar g \alpha_2(t) \hat{x}_L [\hat{\theta}_M \cos(\Omega t) + \hat{L}_M \sin(\Omega t)]$ .

We consider using a short laser to pump the optical mode  $a_2$ , which carries  $N_{\text{in}}$  photons within the duration  $\tau$ . If the condition  $\Omega \ll \tau^{-1} \ll \kappa$  is satisfied, we can reasonably neglect the second term of the Hamiltonian  $H_{\text{OM}}^{\text{new}}$  and obtain the following effective Hamiltonian as [34]

$$H_{\text{eff}} = 2\hbar g \alpha_2(t) \hat{x}_L \hat{\theta}_M. \quad (8)$$

This above Hamiltonian  $H_{\text{eff}}$  describes the effective interaction between the optical mode  $a_1$  and the torsional mode  $b$ . Because of the short pulse characteristic of  $\alpha_2(t)$ , we can define an optomechanical coupling coefficient  $\chi = 4g \sqrt{\int |\alpha_2(t)|^2 dt / \sqrt{\kappa}} \approx 8g \sqrt{N_{\text{in}} / \kappa}$  [34]. More generally, using the optical input-output relation  $a_1^{\text{in}}(t) + a_1^{\text{out}}(t) = \sqrt{\kappa} a_1(t)$ , we can derive the input-output relations [4, 34, 50–53]

$$\begin{aligned} \hat{x}_L^{\text{out}} &= \hat{x}_L^{\text{in}}, \\ \hat{p}_L^{\text{out}} &= \hat{p}_L^{\text{in}} - \chi \hat{\theta}_M^{\text{in}}, \\ \hat{\theta}_M^{\text{out}} &= \hat{\theta}_M^{\text{in}}, \\ \hat{L}_M^{\text{out}} &= \hat{L}_M^{\text{in}} - \chi \hat{x}_L^{\text{in}}. \end{aligned} \quad (9)$$

Through this optomechanical interaction, the optical quadratures  $\hat{x}_L$  and  $\hat{p}_L$  partially exchanges information with the torsional quadratures  $\hat{\theta}_M$  and  $\hat{L}_M$ . Therefore, the quantum state of torsional oscillator becomes correlated with the quantum state of optical mode  $a_1$ .

It can also be seen that, the quantum state of the optical mode  $a_1$  is unaffected by the pumping laser of mode  $a_2$ . As a result, when  $\chi \geq 1$ , Eq.(9) allows an effective coherent control of the torsional oscillator by very few photons of the optical mode  $a_1$ , and thus provides a new platform to realize single photon optomechanics [28], even though this system do not satisfy the usually single photon strong coupling condition  $g \geq \Omega$  [28]. The requirement for the realization of single photon optomechanics, namely to achieve  $\chi \geq 1$  is  $N_{\text{in}} \geq 6.45 \times 10^7$ , which is feasible in the state-of-the art experiment [27, 51].

As powered by the strong single-photon optomechanical coupling with  $\chi \geq 1$ , the torsional oscillator can be squeezed and cooled efficiently in this system using single-pulse-measurement protocol [51]. By using a single coherent pulse to pump mode  $a_2$  and then performing a homodyne detection on quadrature  $\hat{p}_L^{\text{out}}$ , the torsional oscillator will be projected into a state that inherits the features of the input state of the optical mode  $a_1$ . As an example, we assume that the input state of the optical mode  $a_1$  is a vacuum state, and the

input state of the torsional oscillator is a thermal state with the mean phonon number  $\bar{n}$ . According to the input-output relation Eq.(9) and noticing that  $\Delta(\hat{p}_L^{\text{out}})$ , the variance of  $\hat{p}_L^{\text{out}}$  becomes 0 by the homodyne detection, we obtain

$$\begin{aligned} \Delta(\hat{\theta}_M^{\text{out}})^2 &= \chi^{-2} \Delta(\hat{p}_L^{\text{in}})^2 + \chi^{-2} \Delta(\hat{p}_L^{\text{out}})^2 = 1/(2\chi^2), \\ \Delta(\hat{L}_M^{\text{out}})^2 &= \Delta(\hat{L}_M^{\text{in}})^2 + \chi^2 \Delta(\hat{x}_L^{\text{in}})^2 = (\bar{n} + 1/2) + \chi^2/2. \end{aligned} \quad (10)$$

Therefore, when  $\chi \geq 1$ ,  $\Delta(\hat{\theta}_M^{\text{out}})^2 = 1/(2\chi^2) \leq 1/2$ , the  $\hat{\theta}_M$  quadrature is thus squeezed to the level of the vacuum fluctuation and  $\hat{L}_M$  quadrature keeps almost unaffected. As a consequence, this torsional oscillator is squeezed into an asymmetrically cooled state (namely squeezed thermal state) [51, 52] and has a reduced effective phonon number  $\bar{n}_{\text{eff}} = [\Delta(\hat{\theta}_M^{\text{out}})^2 \Delta(\hat{L}_M^{\text{out}})^2]^{1/2} - 1/2 \simeq (\bar{n}/(2\chi^2))^{1/2} \ll \bar{n}$  [51] when  $\bar{n} \gg 1$ .

*Preparation of macroscopic Schrödinger catlike state.*— We proceed to demonstrate that the torsional oscillator can be prepared in a Schrödinger catlike state using a two-pulse-measurement protocol, see Fig.2. The first pulse is used to cool the torsional oscillator, as we have explained before. The second set of pulses includes a coherent laser pulse (to pump

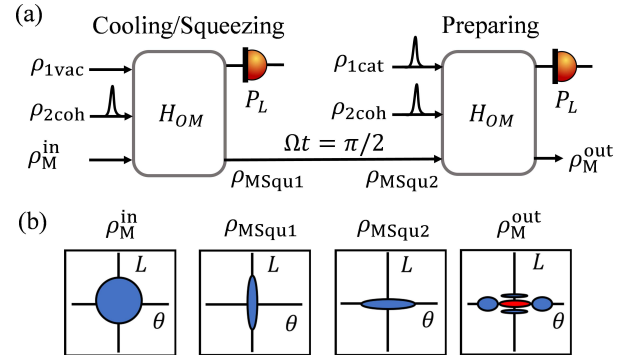


Figure 2. (a) The protocol for the preparation of macroscopic Schrödinger catlike state of the torsional resonator includes three steps: (1) the torsional resonator is cooled and squeezed ( $\rho_M^{\text{in}} \rightarrow \rho_{\text{MSqu1}}$ ) by the first optomechanical interaction  $H_{\text{OM}}$  and the homodyne detection of the  $\hat{p}_L^{\text{out}}$  quadrature of the optical mode  $a_1$  ( $P_L$ ) with the input optical state  $\rho_{1\text{vac}}$  (vacuum state) and  $\rho_{2\text{coh}}$  (coherent state pulse); (2) the free evolution of the torsional resonator for time  $\Omega t = \pi/2$  ( $\rho_{\text{MSqu1}} \rightarrow \rho_{\text{MSqu2}}$ ); (3) the torsional resonator is prepared into a Schrödinger catlike state ( $\rho_{\text{MSqu2}} \rightarrow \rho_M^{\text{out}}$ ) by the second optomechanical interaction  $H_{\text{OM}}$  and the homodyne detection of the optical mode  $a_1$  ( $P_L$ ) with the input optical cat state  $\rho_{1\text{cat}}$  and  $\rho_{2\text{coh}}$  (coherent state pulse). (b) illustrates the Wigner functions of the mechanical state of the torsional resonator during the experimental protocol.

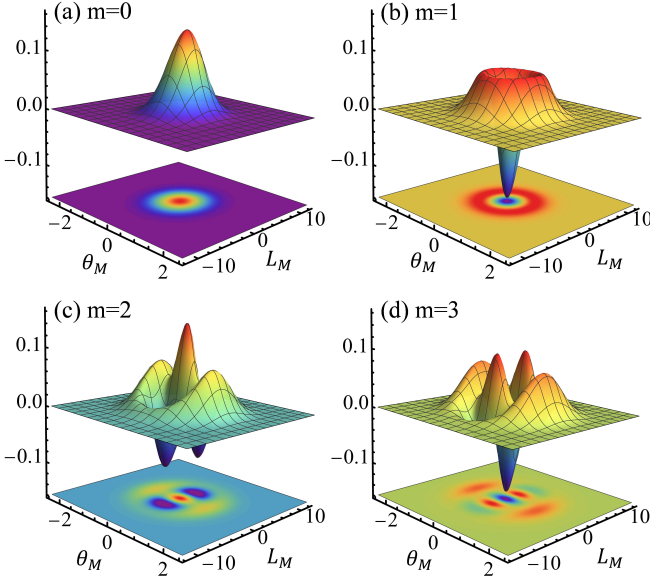


Figure 3. The Wigner functions of the torsional oscillator prepared in Schrödinger catlike states with  $\theta_M$  quadrature squeezed. In our numerical calculation, we choose the coupling coefficient  $\chi = 1$ , the squeezing parameters  $r_1 = -r_2 = 1.15$  (i.e. 10 dB of squeezing),  $T_{\text{tap}} = (e^{2r_1} - 1)/(e^{2r_1} + e^{-2r_1}) \approx 0.909$  [54] and the environment temperature  $T = 100\text{mK}$ . The other parameters we use are listed in Table (I).

the mode  $a_2$ ) and an optical catlike state pulse (i.e. the mode  $a_1$ ) [54]. The subsequent homodyne measurement on the output field  $\hat{p}_L^{\text{out}}$  will partially transfer the quantum state from the optical mode  $a_1$  to the torsional oscillator, thus prepare the torsional oscillator into a Schrödinger catlike state.

We use Wigner function to characterize the state of the torsional oscillator. Given the input optical cat state of mode  $a_1$  with the Wigner function  $W_L(x_L, p_L)$  and a precooled mechanical state with the Wigner function  $W_M(\theta_M, L_M)$ , up to a normalization factor, the Wigner function of the resulting mechanical state  $W(\theta_M, L_M)$  is [34]

$$W(\theta_M, L_M) = \iint dx_L dp_L W_L(x_L, p_L + \chi\theta_M) \times W_M(\theta_M, L_M + \chi x_L) W_{\text{Homo}}(x_L, p_L) \quad (11)$$

where  $W_{\text{Homo}}(x_L, p_L) = \delta(p_L - p)$  is the Wigner function of perfect homodyne measurement [55] and  $p$  is the outcome of the homodyne detection. Following the analysis in [4], we choose  $p = 0$  in our numerical calculation. Eq.(11) describes the quantum state exchanging process between the optical mode  $a_1$  and the torsional oscillator that is induced by the optomechanical interaction (9). The overlap integral between  $W_L(x_L, p_L + \chi\theta_M)$ ,  $W_M(\theta_M, L_M + \chi x_L)$  and  $W_{\text{Homo}}(x_L, p_L)$  describes the process of homodyne detection on the quadrature  $\hat{p}_L^{\text{out}}$ .

Comparing with the macroscopic mechanical cat states which are difficult realized in experiments, the technologies of preparing optical cat state are much more mature [56–58].

Here we use the generalized photon subtraction method [54] to prepare optical cat state. The Wigner function of the prepared optical cat state depends on two squeezing parameter  $r_1, r_2$ , the transmittance  $T_{\text{tap}}$  of an asymmetric beam splitter and the subtracted photon number  $m$ . Using experimental feasible parameters [54], see Table I, the Wigner functions of the resulting mechanical states for  $m = 0, 1, 2, 3$  are plotted in Fig.3. It can be seen that when  $m > 0$ , the Wigner function  $W(\theta_M, L_M)$  for the output state of the torsional oscillator has negative-valued interference fringes between two significantly separated components, which demonstrates the feature of Schrödinger cat state. In addition to the mechanical Schrödinger catlike state, other non-classical quantum states, such as squeezed single phonon fock state, can also be prepared by replacing the input cat state  $\rho_{1\text{cat}}$  with single photon fock state [34].

*Experimental feasibility.*— The torsional oscillator can be implemented by  $\alpha$ -quartz [59], the optical anisotropy may reach  $\delta\epsilon = 0.025$  for  $\lambda = 1.55\mu\text{m}$  [60]. For a suspended square beam with the uniform mass density  $\rho = 2650\text{kg/m}^3$ , the effective moment of inertia is estimated to be  $I_{\text{eff}} \sim 10I_{\text{beam}} = (5/3)\rho a^4 \int_{-L/2}^{L/2} \theta(z)^2 dz = (5/6)\rho L a^4$  [39]. The fundamental mode resonance frequency  $\Omega$  of a torsional oscillator is in the range of  $100\text{kHz} - 1\text{MHz}$  and the mechanical quality factor  $Q_m$  is  $10^3 - 10^4$  [37, 59, 61–63]. In our numerical analysis, we set the cross section width  $a = 1\mu\text{m}$  and the length  $L = 100\mu\text{m}$ . Using the experimentally feasible parameters [34], we estimate that the coupling constant would reach  $g \sim 20\text{kHz}$ .

According to Eq.(6), if  $\theta(z) = \cos(k_t z)$  and  $|\beta_1 - \beta_2| = |\Delta\beta| = k_t \gg L^{-1}$ , we have the coupling constant  $g \propto \delta\epsilon\theta_{zp} \propto \delta\epsilon L^{-1/2}$  [34], where  $k_t = \Omega/c_t$  and the exact acoustic velocity  $c_t$  depends on the cutting direction of this suspended beam [64, 65]. In order to research quantum physics in longer macroscopic scale, we can increase the length  $L$  from  $0.1\text{mm}$  to  $1\text{cm}$ , e.g. with a centimeter-long optical cavity on a nanofiber [32], then the coupling constant  $g$  will reduce by an order of magnitude, which can be compensated by using the optical material with a higher optical anisotropy  $\delta\epsilon$  as compared with  $\alpha$ -quartz, such as  $\text{TiO}_2$  ( $\delta\epsilon \approx 1.536$ ) [66] and  $\text{YVO}_4$  ( $\delta\epsilon \approx 0.936$ ) [67] for  $\lambda = 0.63\mu\text{m}$ . We note that the optical quality factor  $Q_o$  on the order of  $10^5 - 10^7$  can be achieved by using photonic crystal mirror [32, 68, 69]. Therefore, it is possible to realize strong spin angular momentum optomechanical coupling for a centimeter long torsional oscillator, and prepare the torsional oscillator in Schrödinger catlike state using a nanofiber cavity with anisotropic permittivity [70] to serve as the optomechanical resonator.

*Conclusion.*— We have theoretically proposed a novel optomechanical system which is based on spin angular momentum exchange interaction between light and a torsional oscillator. Our analysis shows that this system can be used to manipulate the torsional quantum state of a torsional oscillator and prepare Schrödinger catlike states with macroscopic length scale. These results pave a feasible route towards the



long-standing goal of interrogating quantum mechanical phenomena at the macroscopic scale. Furthermore, the combination of the present optomechanical system with solid spin system [71] or atomic system [72, 73] may provide a new platform of hybrid quantum optomechanics, e.g. to investigate non-demolition measurement of the phonon energy [71], sympathetic cooling of a mechanical oscillator [72], creation of a robust EPR-type of entanglement [74] between atomic ensemble and a mechanical resonator [75].

*Acknowledgements.*— We thank Dr. Ralf Betzholtz for helpful discussions. This work is supported by National Natural Science Foundation of China (Grant No. 11874024, 11690032, 12047525), the Open Project Program of Wuhan National Laboratory for Optoelectronics (2019WNLOKF002), and the Fundamental Research Funds for the Central Universities.

\* shaoliang@hust.edu.cn

† jianmingcai@hust.edu.cn

- [1] F. Marquardt, J. P. Chen, A. A. Clerk, and S. M. Girvin, Quantum theory of cavity-assisted sideband cooling of mechanical motion, *Phys. Rev. Lett.* **99**, 093902 (2007).
- [2] A. Schliesser, P. Del’Haye, N. Nooshi, K. J. Vahala, and T. J. Kippenberg, Radiation pressure cooling of a micromechanical oscillator using dynamical backaction, *Phys. Rev. Lett.* **97**, 243905 (2006).
- [3] I. Wilson-Rae, N. Nooshi, W. Zwerger, and T. J. Kippenberg, Theory of ground state cooling of a mechanical oscillator using dynamical backaction, *Phys. Rev. Lett.* **99**, 093901 (2007).
- [4] U. B. Hoff, J. Kollath-Bönig, J. S. Neergaard-Nielsen, and U. L. Andersen, Measurement-induced macroscopic superposition states in cavity optomechanics, *Phys. Rev. Lett.* **117**, 143601 (2016).
- [5] J. Li, S. Gröblacher, S.-Y. Zhu, and G. S. Agarwal, Generation and detection of non-gaussian phonon-added coherent states in optomechanical systems, *Phys. Rev. A* **98**, 011801 (2018).
- [6] R. Y. Teh, S. Kiesewetter, P. D. Drummond, and M. D. Reid, Creation, storage, and retrieval of an optomechanical cat state, *Phys. Rev. A* **98**, 063814 (2018).
- [7] U. Akram, W. P. Bowen, and G. J. Milburn, Entangled mechanical cat states via conditional single photon optomechanics, *New Journal of Physics* **15**, 093007 (2013).
- [8] I. Wilson-Rae, N. Nooshi, W. Zwerger, and T. J. Kippenberg, Theory of ground state cooling of a mechanical oscillator using dynamical backaction, *Phys. Rev. Lett.* **99**, 093901 (2007).
- [9] A. Schliesser, P. Del’Haye, N. Nooshi, K. J. Vahala, and T. J. Kippenberg, Radiation pressure cooling of a micromechanical oscillator using dynamical backaction, *Phys. Rev. Lett.* **97**, 243905 (2006).
- [10] G.ENZIAN, J. J. Price, L. Freisem, J. Nunn, J. Janousek, B. C. Buchler, P. K. Lam, and M. R. Vanner, Single-phonon addition and subtraction to a mechanical thermal state, *Phys. Rev. Lett.* **126**, 033601 (2021).
- [11] J. Li, S. Gröblacher, S.-Y. Zhu, and G. S. Agarwal, Generation and detection of non-gaussian phonon-added coherent states in optomechanical systems, *Phys. Rev. A* **98**, 011801 (2018).
- [12] E. Schrödinger, Die gegenwärtige situation in der quantenmechanik, *Naturwissenschaften* **23**, 807 (1935).
- [13] F. Fröwis, P. Sekatski, W. Dür, N. Gisin, and N. Sangouard, Macroscopic quantum states: Measures, fragility, and implementations, *Rev. Mod. Phys.* **90**, 025004 (2018).
- [14] A. Bassi, K. Lochan, S. Satin, T. P. Singh, and H. Ulbricht, Models of wave-function collapse, underlying theories, and experimental tests, *Rev. Mod. Phys.* **85**, 471 (2013).
- [15] V. Garcés-Chávez, K. Volke-Sepulveda, S. Chávez-Cerda, W. Sibbett, and K. Dholakia, Transfer of orbital angular momentum to an optically trapped low-index particle, *Phys. Rev. A* **66**, 063402 (2002).
- [16] M. E. J. Friese, J. Enger, H. Rubinsztein-Dunlop, and N. R. Heckenberg, Optical angular-momentum transfer to trapped absorbing particles, *Phys. Rev. A* **54**, 1593 (1996).
- [17] H. Adachi, S. Akahoshi, and K. Miyakawa, Orbital motion of spherical microparticles trapped in diffraction patterns of circularly polarized light, *Phys. Rev. A* **75**, 063409 (2007).
- [18] M. E. J. Friese, T. A. Nieminen, N. R. Heckenberg, and H. Rubinsztein-Dunlop, Optical alignment and spinning of laser-trapped microscopic particles, *Nature* **394**, 348 (1998).
- [19] L. Paterson, M. P. MacDonald, J. Arlt, W. Sibbett, P. E. Bryant, and K. Dholakia, Controlled rotation of optically trapped microscopic particles, *Science* **292**, 912 (2001).
- [20] M. Bhattacharya and P. Meystre, Using a laguerre-gaussian beam to trap and cool the rotational motion of a mirror, *Phys. Rev. Lett.* **99**, 153603 (2007).
- [21] T. M. Hoang, Y. Ma, J. Ahn, J. Bang, F. Robicheaux, Z.-Q. Yin, and T. Li, Torsional optomechanics of a levitated nonspherical nanoparticle, *Phys. Rev. Lett.* **117**, 123604 (2016).
- [22] R. Reimann, M. Doderer, E. Hebestreit, R. Diehl, M. Frimmer, D. Windey, F. Tebbenjohanns, and L. Novotny, Ghz rotation of an optically trapped nanoparticle in vacuum, *Phys. Rev. Lett.* **121**, 033602 (2018).
- [23] J. Ahn, Z. Xu, J. Bang, P. Ju, X. Gao, and T. Li, Ultrasensitive torque detection with an optically levitated nanorotor, *Nature Nanotechnology* **15**, 89 (2020).
- [24] E. F. Fenton, A. Khan, P. Solano, L. A. Orozco, and F. K. Fatemi, Spin-optomechanical coupling between light and a nanofiber torsional mode, *Opt. Lett.* **43**, 1534 (2018).
- [25] L. He, H. Li, and M. Li, Optomechanical measurement of photon spin angular momentum and optical torque in integrated photonic devices, *Science Advances* **2**, 10.1126/sciadv.1600485 (2016).
- [26] M. Dakna, T. Anhut, T. Opatrny, L. Knöll, and D.-G. Welsch, Generating schrödinger-cat-like states by means of conditional measurements on a beam splitter, *Phys. Rev. A* **55**, 3184 (1997).
- [27] J. T. Muhonen, G. R. La Gala, R. Leijssen, and E. Verhagen, State preparation and tomography of a nanomechanical resonator with fast light pulses, *Phys. Rev. Lett.* **123**, 113601 (2019).
- [28] A. Nunnenkamp, K. Børkje, and S. M. Girvin, Single-photon optomechanics, *Phys. Rev. Lett.* **107**, 063602 (2011).
- [29] C. Zhong and F. Robicheaux, Decoherence of rotational degrees of freedom, *Phys. Rev. A* **94**, 052109 (2016).
- [30] B. A. Stickler, B. Schriniski, and K. Hornberger, Rotational friction and diffusion of quantum rotors, *Phys. Rev. Lett.* **121**, 040401 (2018).
- [31] T. H. Stievater, M. W. Pruessner, W. S. Rabinovich, D. Park, R. Mahon, D. A. Kozak, J. B. Boos, S. A. Holmstrom, and J. B. Khurgin, Suspended photonic waveguide devices, *Appl. Opt.* **54**, F164 (2015).
- [32] J. Keloth, K. P. Nayak, and K. Hakuta, Fabrication of a centimeter-long cavity on a nanofiber for cavity quantum electrodynamics, *Opt. Lett.* **42**, 1003 (2017).
- [33] Q. Qiao, J. Xia, C. Lee, and G. Zhou, Applications of photonic crystal nanobeam cavities for sensing, *Micromachines* **9**,

- 10.3390/mi9110541 (2018).
- [34] See Supplemental Material for further experiment details, which includes Refs..
  - [35] F. Le Kien and K. Hakuta, Cavity-enhanced channeling of emission from an atom into a nanofiber, *Phys. Rev. A* **80**, 053826 (2009).
  - [36] F. Le Kien and K. Hakuta, Effect of an atom on a quantum guided field in a weakly driven fiber-bragg-grating cavity, *Phys. Rev. A* **81**, 023812 (2010).
  - [37] C. Wuttke, G. D. Cole, and A. Rauschenbeutel, Optically active mechanical modes of tapered optical fibers, *Phys. Rev. A* **88**, 061801 (2013).
  - [38] H. E. Engan, B. Y. Kim, J. N. Blake, and H. J. Shaw, Propagation and optical interaction of guided acoustic waves in two-mode optical fibers, *Journal of Lightwave Technology* **6**, 428 (1988).
  - [39] C. Wuttke, *Thermal excitations of optical nanofibers measured with a cavity*, Ph.D. thesis, Ph. D. dissertation (University of Mainz, 2014) (2014).
  - [40] J. D. Jackson, *Classical electrodynamics* (1999).
  - [41] A. Yariv and P. Yeh, *Optical waves in crystals*, Vol. 5 (Wiley New York, 1984).
  - [42] H. Zoubi and K. Hammerer, Optomechanical multimode hamiltonian for nanophotonic waveguides, *Phys. Rev. A* **94**, 053827 (2016).
  - [43] S. G. Johnson, M. Ibanescu, M. A. Skorobogatiy, O. Weisberg, J. D. Joannopoulos, and Y. Fink, Perturbation theory for maxwell's equations with shifting material boundaries, *Phys. Rev. E* **65**, 066611 (2002).
  - [44] M. Ludwig, A. H. Safavi-Naeini, O. Painter, and F. Marquardt, Enhanced quantum nonlinearities in a two-mode optomechanical system, *Phys. Rev. Lett.* **109**, 063601 (2012).
  - [45] R. Burgwal, J. del Pino, and E. Verhagen, Comparing nonlinear optomechanical coupling in membrane-in-the-middle and single-cavity systems, *New Journal of Physics* **22**, 113006 (2020).
  - [46] P. Kómár, S. D. Bennett, K. Stannigel, S. J. M. Habraken, P. Rabl, P. Zoller, and M. D. Lukin, Single-photon nonlinearities in two-mode optomechanics, *Phys. Rev. A* **87**, 013839 (2013).
  - [47] J. Chan, T. P. M. Alegre, A. H. Safavi-Naeini, J. T. Hill, A. Krause, S. Gröblacher, M. Aspelmeyer, and O. Painter, Laser cooling of a nanomechanical oscillator into its quantum ground state, *Nature* **478**, 89 (2011).
  - [48] C. Schäfermeier, H. Kerdoncuff, U. B. Hoff, H. Fu, A. Huck, J. Bilek, G. I. Harris, W. P. Bowen, T. Gehring, and U. L. Andersen, Quantum enhanced feedback cooling of a mechanical oscillator using nonclassical light, *Nature Communications* **7**, 13628 (2016).
  - [49] J. Wang, Y. Shi, and S. Fan, Non-reciprocal polarization rotation using dynamic refractive index modulation, *Opt. Express* **28**, 11974 (2020).
  - [50] J. S. Bennett, K. Khosla, L. S. Madsen, M. R. Vanner, H. Rubinsztein-Dunlop, and W. P. Bowen, A quantum optomechanical interface beyond the resolved sideband limit, *New Journal of Physics* **18**, 053030 (2016).
  - [51] M. R. Vanner, J. Hofer, G. D. Cole, and M. Aspelmeyer, Cooling-by-measurement and mechanical state tomography via pulsed optomechanics, *Nature Communications* **4**, 2295 (2013).
  - [52] M. R. Vanner, I. Pikovski, G. D. Cole, M. S. Kim, Č. Brukner, K. Hammerer, G. J. Milburn, and M. Aspelmeyer, Pulsed quantum optomechanics, *Proceedings of the National Academy of Sciences* **108**, 16182 (2011).
  - [53] B. Julsgaard, J. Sherson, J. I. Cirac, J. Fiurášek, and E. S. Polzik, Experimental demonstration of quantum memory for light, *Nature* **432**, 482 (2004).
  - [54] K. Takase, J.-i. Yoshikawa, W. Asavanant, M. Endo, and A. Furusawa, Generation of optical schrödinger cat states by generalized photon subtraction, *Phys. Rev. A* **103**, 013710 (2021).
  - [55] A. Ferraro, S. Olivares, and M. G. A. Paris, Gaussian states in continuous variable quantum information, (2005), [arXiv:quant-ph/0503237](https://arxiv.org/abs/quant-ph/0503237).
  - [56] M. Takeoka, H. Takahashi, and M. Sasaki, Large-amplitude coherent-state superposition generated by a time-separated two-photon subtraction from a continuous-wave squeezed vacuum, *Phys. Rev. A* **77**, 062315 (2008).
  - [57] H. Takahashi, K. Wakui, S. Suzuki, M. Takeoka, K. Hayasaka, A. Furusawa, and M. Sasaki, Generation of large-amplitude coherent-state superposition via ancilla-assisted photon subtraction, *Phys. Rev. Lett.* **101**, 233605 (2008).
  - [58] L. Duan, Creating schrödinger-cat states, *Nature Photonics* **13**, 73 (2019).
  - [59] Y.-I. Sohn, R. Miller, V. Venkataraman, and M. Lončar, Mechanical and optical nanodevices in single-crystal quartz, *Applied Physics Letters* **111**, 263103 (2017).
  - [60] G. Ghosh, Dispersion-equation coefficients for the refractive index and birefringence of calcite and quartz crystals, *Optics Communications* **163**, 95 (1999).
  - [61] L. He, H. Li, and M. Li, Optomechanical measurement of photon spin angular momentum and optical torque in integrated photonic devices, *Science Advances* **2**, 10.1126/sciadv.1600485 (2016).
  - [62] B. Kim, J. Jahng, R. M. Khan, S. Park, and E. O. Potma, Eigenmodes of a quartz tuning fork and their application to photoinduced force microscopy, *Phys. Rev. B* **95**, 075440 (2017).
  - [63] R. O. Pohl, X. Liu, and E. Thompson, Low-temperature thermal conductivity and acoustic attenuation in amorphous solids, *Rev. Mod. Phys.* **74**, 991 (2002).
  - [64] H. Kawashima and K. Sunaga, Torsional vibrations of quartz crystal beams, *IEEE Transactions on Ultrasonics, Ferroelectrics, and Frequency Control* **43**, 832 (1996).
  - [65] J.-i. Kushibiki, M. Ohtagawa, and I. Takanaga, Comparison of acoustic properties between natural and synthetic  $\alpha$ -quartz crystals, *Journal of Applied Physics* **94**, 295 (2003).
  - [66] J. R. DeVore, Refractive indices of rutile and sphalerite, *J. Opt. Soc. Am.* **41**, 416 (1951).
  - [67] T. S. Lomheim and L. G. DeShazer, Optical-absorption intensities of trivalent neodymium in the uniaxial crystal yttrium orthovanadate, *Journal of Applied Physics* **49**, 5517 (1978).
  - [68] P. B. Deotare, M. W. McCutcheon, I. W. Frank, M. Khan, and M. Lončar, High quality factor photonic crystal nanobeam cavities, *Applied Physics Letters* **94**, 121106 (2009).
  - [69] Q. Quan and M. Loncar, Deterministic design of wavelength scale, ultra-high q photonic crystal nanobeam cavities, *Opt. Express* **19**, 18529 (2011).
  - [70] A. W. Snyder and F. Rühl, Single-mode, single-polarization fibers made of birefringent material, *J. Opt. Soc. Am.* **73**, 1165 (1983).
  - [71] B. D'Urso, M. V. G. Dutt, S. Dhirga, and N. M. Nusran, Quantum measurements between a single spin and a torsional nanomechanical resonator, *New Journal of Physics* **13**, 045002 (2011).
  - [72] A. Jöckel, A. Faber, T. Kampschulte, M. Korppi, M. T. Rakher, and P. Treutlein, Sympathetic cooling of a membrane oscillator in a hybrid mechanical-atomic system, *Nature Nanotechnology* **10**, 55 (2015).
  - [73] W. S. Leong, M. Xin, Z. Chen, S. Chai, Y. Wang, and S.-Y. Lan, Large array of schrödinger cat states facilitated by an optical waveguide, *Nature Communications* **11**, 5295 (2020).
  - [74] S. L. Braunstein and P. van Loock, Quantum information with

- continuous variables, [Rev. Mod. Phys. 77, 513 \(2005\)](#).
- [75] K. Hammerer, M. Aspelmeyer, E. S. Polzik, and P. Zoller, Establishing einstein-poldosky-rosen channels between nanomechanics and atomic ensembles, [Phys. Rev. Lett. 102, 020501 \(2009\)](#).

# Supplementary

## CONTENTS

I. Angular Momentum Optomechanical Interaction	2
A. Moving Boundary Coupling Effect	3
B. Opto-elastic Coupling Effect and Optical Material Anisotropy Coupling Effect	3
1. Optical Material Anisotropy Coupling Effect	3
2. Opto-elastic Coupling Effect	4
3. Expression of $\epsilon_{\text{other}}$	4
C. Quantization of The Optomechanical Hamiltonian	4
D. Discussion About the Torsional Oscillator	5
E. Calculation of the Coupling Constants	5
F. A Simple Explanation For Our Optomechanical Hamiltonian	7
II. Discussion about input-output relation	8
A. Mechanical Mode	8
B. Optical Mode $a_2$	9
C. Input-Output Relation	9
III. Wigner Function Formaluism	10
A. General Definition of Wigner function	10
B. Time evolution of Wigner function	11
C. The Resulting Wigner Function	11
References	14



## I. ANGULAR MOMENTUM OPTOMECHANICAL INTERACTION

In this section we discuss the optomechanical Hamiltonian. Firstly, we derive the classical Hamiltonian that represents the mutual influence of the mechanical motion and the electromagnetic field in a bounded dielectric medium, which are characterized by the electric field  $\mathbf{E}(\mathbf{x})$  and the mechanical displacement field  $\mathbf{Q}(\mathbf{x})$ , respectively. For simplify we assume that  $\mathbf{Q}(\mathbf{x}) = \alpha \mathbf{u}(\mathbf{x})$ , where  $\mathbf{u}(\mathbf{x})$  is the mode function of the mechanical displacement, which satisfies the condition that  $\max |\mathbf{u}| = 1$  and  $\alpha$  is the amplitude of the mechanical displacement. Usually  $\alpha$  is much smaller than the scale of the mechanical oscillator. By quantizing the classical electromagnetic Hamiltonian, we can derive the optomechanical Hamiltonian.

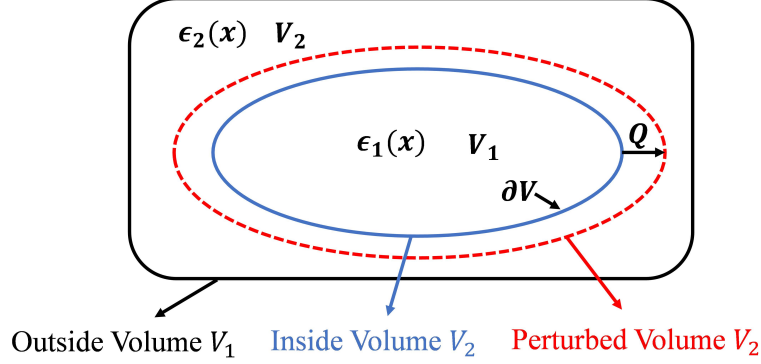


Figure 1. A dielectric material with permittivity  $\epsilon_1$  in a volume  $V_1$  (blue circle) is surrounded by a medium with permittivity  $\epsilon_2$  occupying the complementary volume  $V_2$  (black circle). The perturbed volume is represented by the dashed red circle and  $\mathbf{Q}$  is the corresponding mechanical displacement.  $\partial V$  is the boundary between  $V_1$  and  $V_2$ .

We consider a dielectric material with permittivity  $\epsilon(\mathbf{x}) = \epsilon_1$  in a volume  $V_1$ , which is localized in a surrounding medium with permittivity  $\epsilon(\mathbf{x}) = \epsilon_2$  occupying the complementary volume  $V_2$ . For a dielectric material in vacuum  $\epsilon_2 = \epsilon_0$ . The unperturbed permittivity can be written as

$$\epsilon(\mathbf{x}) = \epsilon_2 + (\epsilon_1 - \epsilon_2) \Theta(\mathbf{x}) \quad (1)$$

where  $\Theta(\mathbf{x})$  is a step function defined by

$$\Theta(\mathbf{x}) = \begin{cases} 1 & \text{for } \mathbf{x} \in V_1 \\ 0 & \text{for } \mathbf{x} \in V_2 \end{cases} \quad (2)$$

The mechanical motion of the dielectric material will influence the total permittivity  $\epsilon(\mathbf{x})$ . We assume that  $\epsilon_1 = \epsilon_1(\mathbf{x}, \mathbf{Q}(\mathbf{x})) = \epsilon_1(\mathbf{x}, \alpha)$ , which is also dependent on  $\mathbf{Q}(\mathbf{x})$ . Notice that when  $\alpha = 0$ ,  $\epsilon_1(\mathbf{x}, \alpha)|_{\alpha=0} = \epsilon_1(\mathbf{x}, 0)$ , which is the unperturbed value. The perturbed permittivity induced by mechanical displacement  $\mathbf{Q}$  can be written as

$$\epsilon(\mathbf{x}, \alpha) = \epsilon_2 + [\epsilon_1(\mathbf{x}, \mathbf{Q}) - \epsilon_2] \Theta(\mathbf{x} + \mathbf{Q}) = \epsilon_2 + [\epsilon_1(\mathbf{x}, \alpha) - \epsilon_2] \Theta(\mathbf{x} + \alpha \mathbf{u}). \quad (3)$$

Expanding  $\epsilon(\mathbf{x}, \alpha)$  to the first order of  $\alpha$ ,  $\epsilon(\mathbf{x}, \alpha)$  is

$$\begin{aligned} \epsilon(\mathbf{x}, \alpha) &\approx \epsilon_2 + \left[ \epsilon_1(\mathbf{x}, 0) - \epsilon_2 + \alpha \frac{\partial \epsilon_1(\mathbf{x}, \alpha)}{\partial \alpha} \bigg|_{\alpha=0} \right] [\Theta(\mathbf{x}) + \alpha \mathbf{u}(\mathbf{x}) \cdot \nabla \Theta(\mathbf{x})] \\ &\approx \epsilon_2 + [\epsilon_1(\mathbf{x}, 0) - \epsilon_2] \Theta(\mathbf{x}) + \alpha (\epsilon_1(\mathbf{x}, 0) - \epsilon_2) \mathbf{u}(\mathbf{x}) \cdot \nabla \Theta(\mathbf{x}) + \alpha \frac{\partial \epsilon_1(\mathbf{x}, \alpha)}{\partial \alpha} \bigg|_{\alpha=0} \Theta(\mathbf{x}) \\ &= \epsilon(\mathbf{x}) + \alpha (\epsilon_{MB} + \epsilon_{other}) \end{aligned} \quad (4)$$

where  $\epsilon_{MB} = (\epsilon_1(\mathbf{x}, 0) - \epsilon_2) \mathbf{u}(\mathbf{x}) \cdot \nabla \Theta(\mathbf{x})$  is the moving boundary effect ( $\mathbf{u} \cdot \nabla \Theta(\mathbf{x})$ ) induced permittivity and  $\epsilon_{other} = \frac{\partial \epsilon_1(\mathbf{x}, \alpha)}{\partial \alpha} \bigg|_{\alpha=0} \Theta(\mathbf{x})$  is other effects induced permittivity. Considering the electromagnetic Hamiltonian  $H_{em}$  is  $H_{em} = 1/2 \int_V dV (\mathbf{E}(\mathbf{x}) \cdot \epsilon(\mathbf{x}) \mathbf{E}(\mathbf{x}) + \mathbf{H}(\mathbf{x}) \cdot \mu(\mathbf{x}) \mathbf{H}(\mathbf{x}))$ , we can easily derive the optomechanical coupling Hamiltonian  $H_{MB}$  and  $H_{other}$ ,

$$H_{MB} = \frac{1}{2} \alpha \int dV \mathbf{E}(\mathbf{x})^\dagger \epsilon_{MB} \mathbf{E}(\mathbf{x}), \quad (5)$$

$$H_{\text{other}} = \frac{1}{2}\alpha \int dV \mathbf{E}(\mathbf{x})^\dagger \epsilon_{\text{other}} \mathbf{E}(\mathbf{x}). \quad (6)$$

In following subsections we will mainly discuss  $H_{MB}$  and  $H_{\text{other}}$ .

### A. Moving Boundary Coupling Effect

If the boundary of an optical resonator is perturbed by the motion of a mechanical resonator, the energy of the total electromagnetic field will be perturbed, which can be understood from the expression  $\epsilon_{MB} \propto \mathbf{u}(\mathbf{x}) \cdot \Theta(\mathbf{x})$ . By means of simple mathematical transformations,  $H_{MB}$  can be expressed as

$$H_{MB} = \frac{1}{2}\alpha \int_{\partial V} d\mathbf{A} \cdot \mathbf{u}(\mathbf{x}) \{ -\mathbf{E}_{\parallel}(\mathbf{x})^\dagger \Delta \epsilon \mathbf{E}_{\parallel}(\mathbf{x}) + \mathbf{D}_{\perp}(\mathbf{x})^\dagger \Delta(\epsilon^{-1}) \mathbf{D}_{\perp}(\mathbf{x}) \} \quad (7)$$

where  $\Delta \epsilon = \epsilon_1 - \epsilon_2$ ,  $\Delta(\epsilon^{-1}) = \epsilon_1^{-1} - \epsilon_2^{-1}$ ,  $\mathbf{E}_{\parallel}$  is the electric field which is parallel with the surface of  $V_1$  and  $\mathbf{D}_{\perp}$  is the electric displacement field which is perpendicular with the surface of  $V_1$ . The detailed calculation process can be found in references [1, 2].

### B. Opto-elastic Coupling Effect and Optical Material Anisotropy Coupling Effect

In this section we mainly discuss the permittivity  $\epsilon_{\text{other}} = \left. \frac{\partial \epsilon_1(\mathbf{Q})}{\partial \alpha} \right|_{\alpha=0} \Theta(\mathbf{x})$ . Function  $\Theta(\mathbf{x})$  shows that  $\epsilon_{\text{other}}$  can only be non-zero in the region of  $V_1$ , which means that Hamiltonian  $H_{\text{other}}$  is concentrated in the region of optomechanical resonator.

#### 1. Optical Material Anisotropy Coupling Effect

We assume that the material of the optical resonator is optical anisotropy, when mechanical displacement  $\alpha = 0$ , the unperturbed permittivity  $\epsilon_1$  can be expressed as a diagonal matrix

$$\epsilon_1(\mathbf{x}, 0) = \begin{pmatrix} \epsilon_{xx} & 0 & 0 \\ 0 & \epsilon_{yy} & 0 \\ 0 & 0 & \epsilon_{zz} \end{pmatrix}, \quad (8)$$

where  $\epsilon_{ii}$  ( $i=x,y,z$ ) is the permittivity along  $i$  axis. In our main article, the displacement vector  $\mathbf{u}(\mathbf{x})$  of the torsional motion is given by  $\mathbf{u}(\mathbf{x}) = \theta(z)(r/R)\hat{\boldsymbol{\theta}} = \theta(z)(-y\hat{\mathbf{x}} + x\hat{\mathbf{y}})/R$  in cylindrical and Cartesian coordinates, respectively. Here  $R$  makes  $\mathbf{u}$  satisfies the condition  $\max |\mathbf{u}| = 1$  and  $\theta(z)$  is the spatial mode function of torsional motion and satisfies the condition  $\max |\theta(z)| = 1$ .

In lab frame, the rotation of the optical material will influence  $\epsilon_1$ ,

$$\epsilon_1(\mathbf{x}, \alpha) = R(\alpha\theta(z))\epsilon_1(0)R(-\alpha\theta(z)), \quad (9)$$

where  $R(\alpha)$  is a rotation matrix,

$$R(\alpha) = \begin{pmatrix} \cos(\alpha) & -\sin(\alpha) & 0 \\ \sin(\alpha) & \cos(\alpha) & 0 \\ 0 & 0 & 1 \end{pmatrix}. \quad (10)$$

If  $\alpha \ll 1$ ,  $R(\alpha)$  can be expanded into  $R(\alpha) = I + \alpha T$ , where  $T$  is

$$T = \begin{pmatrix} 0 & -1 & 0 \\ 1 & 0 & 0 \\ 0 & 0 & 0 \end{pmatrix}. \quad (11)$$

Expanding  $\epsilon_1(\mathbf{x}, \alpha)$  to the first order of  $\alpha$ , we have

$$\epsilon_1(\mathbf{x}, \alpha) \approx \epsilon_1(\mathbf{x}, 0) + \alpha\theta(z)[T, \epsilon_1(\mathbf{x}, 0)] = \epsilon_1(\mathbf{x}, 0) + \alpha\theta(z)\delta\epsilon A \quad (12)$$

where  $\delta\epsilon = \epsilon_{xx} - \epsilon_{yy}$  and  $A = \begin{pmatrix} 0 & 1 & 0 \\ 1 & 0 & 0 \\ 0 & 0 & 0 \end{pmatrix}$ .

## 2. Opto-elastic Coupling Effect

The refractive index of most material will be influenced by opto-elastic effect when material is subject to strain. Mathematically, the opto-elastic effect is described by relating the change of the permittivity tensor  $\delta\eta$ , to the material strain by Pockel's tensor  $p$  [3],  $(\delta\eta)_{ij} = p_{ijkl}s_{kl}$ , where  $s_{mn}$  is the strain tensor of the material with  $s_{mn} = \frac{1}{2} \left( \frac{\partial \mathbf{u}_m}{\partial \mathbf{x}_n} + \frac{\partial \mathbf{u}_n}{\partial \mathbf{x}_m} \right)$ . The modified permittivity tensor follows from  $\epsilon^{OE} = (\epsilon^{-1} + \alpha\delta\eta)^{-1}$ , where  $\epsilon$  is the unmodified permittivity tensor. Considering equation (9), the final expression of  $\epsilon_1^{OE}(\mathbf{x}, \alpha)$  is

$$\begin{aligned} \epsilon_1^{OE}(\mathbf{x}, \alpha) &= (\epsilon_1(\mathbf{x}, \alpha)^{-1} + \alpha\delta\eta)^{-1} \\ &= (R(\alpha\theta)\epsilon_1^{-1}(\mathbf{x}, 0)R(-\alpha\theta) + \alpha\delta\eta)^{-1} \\ &\approx ((I + \alpha\theta T)\epsilon_1^{-1}(\mathbf{x}, 0)(I - \alpha\theta T) + \alpha\delta\eta)^{-1} \\ &\approx (\epsilon_1^{-1}(\mathbf{x}, 0) + \alpha\theta(T\epsilon_1^{-1}(\mathbf{x}, 0) - \epsilon_1^{-1}(\mathbf{x}, 0)T) + \alpha\delta\eta)^{-1} \\ &\approx \epsilon_1(\mathbf{x}, 0) + \alpha\theta\delta\epsilon A - \alpha\epsilon_1(\mathbf{x}, 0)\delta\eta\epsilon_1(\mathbf{x}, 0). \end{aligned} \quad (13)$$

## 3. Expression of $\epsilon_{other}$

The final expression of  $\epsilon_{other}$  is

$$\begin{aligned} \epsilon_{other} &= \frac{\partial \epsilon_1(\mathbf{Q})}{\partial \alpha} \Theta(\mathbf{x}) \\ &= \theta[T, \epsilon_1(\mathbf{x}, 0)]\Theta(\mathbf{x}) - \epsilon_1(\mathbf{x}, 0)\delta\eta\epsilon_1(\mathbf{x}, 0)\Theta(\mathbf{x}) \\ &= \epsilon_{MA} + \epsilon_{OE}. \end{aligned} \quad (14)$$

The first term  $\epsilon_{MA} = \theta[T, \epsilon_1(\mathbf{x}, 0)]\Theta(\mathbf{x}) = \theta\delta\epsilon A\Theta(\mathbf{x})$  is related with the optical anisotropy of the material and the second term  $\epsilon_{OE} = -\epsilon_1(\mathbf{x}, 0)\delta\eta\epsilon_1(\mathbf{x}, 0)\Theta(\mathbf{x})$  is related with opto-elastic effect. Therefore, the optomechanical Hamiltonian  $H_{other}$  can be divided into two terms  $H_{AM}$  and  $H_{OE}$ ,

$$H_{OE} = -\frac{1}{2}\alpha \int_{V_1} dV \mathbf{E}(\mathbf{x})^\dagger \epsilon_1(\mathbf{x}, 0)\delta\eta\epsilon_1(\mathbf{x}, 0)\mathbf{E}(\mathbf{x}), \quad (15)$$

$$H_{MA} = \frac{1}{2}\alpha\delta\epsilon \int_{V_1} dV \theta(z)\mathbf{E}(\mathbf{x})^\dagger A\mathbf{E}(\mathbf{x}). \quad (16)$$

## C. Quantization of The Optomechanical Hamiltonian

The quantized optomechanical Hamiltonian is obtained from the classical one by replacing the classical amplitude  $\alpha$  and the electromagnetic fields by operators. We define  $x_{zp} = \sqrt{\hbar/(2m_{\text{eff}}\Omega)}$  is the zero point linear displacement of the torsional oscillator, where  $m_{\text{eff}} = \int_V |\mathbf{u}(\mathbf{x})|^2 \rho dV$  is the effective mass, and  $\theta_{zp} = \sqrt{\hbar/(2I_{\text{eff}}\Omega)}$  is the effective zero point angular displacement of the torsional oscillator and  $I_{\text{eff}}$  is the effective moment of inertia of the torsional oscillator. For a two mode electric field  $\mathbf{E} = \mathbf{E}_1 a_1 + \mathbf{E}_2 a_2 + h.c.$  ( $\vec{E}_1$  and  $\vec{E}_2$  are not normalized), the original optomechanical Hamiltonian  $H_{\text{int}}$  is

$$H_{\text{int}} = H_{MB} + H_{OE} + H_{MA} = \hbar(b + b^\dagger) \sum_{i,j=1,2} a_i^\dagger a_j g_{ij} \quad (17)$$

where  $g_{ij} = g_{ijMB} + g_{ijOE} + g_{ijAM}$  and

$$\begin{aligned} g_{ijMB} &= \frac{x_{zp}}{2} \int_{\partial V} d\mathbf{A} \cdot \mathbf{u}(\mathbf{x}) \{ -\mathbf{E}_{i\parallel}(\mathbf{x})^\dagger \Delta \epsilon \mathbf{E}_{j\parallel}(\mathbf{x}) + \mathbf{D}_{i\perp}(\mathbf{x})^\dagger \Delta(\epsilon^{-1}) \mathbf{D}_{j\perp}(\mathbf{x}) \}, \\ g_{ijOE} &= -\frac{x_{zp}}{2} \int_{V_1} dV \mathbf{E}_i(\mathbf{x})^\dagger \epsilon_1(\mathbf{x}, 0)\delta\eta\epsilon_1(\mathbf{x}, 0)\mathbf{E}_j(\mathbf{x}), \\ g_{ijMA} &= \frac{1}{2}\theta_{zp}\delta\epsilon \int_{V_1} dV \theta(z) (E_{iy}(\mathbf{x})E_{jx}^*(\mathbf{x}) + E_{jy}^*(\mathbf{x})E_{ix}(\mathbf{x})). \end{aligned} \quad (18)$$

Here we use "MB" to represent moving-boundary coupling effect, use "OE" to represent opto-elastic coupling effect and use "MA" to represent material anisotropy coupling effect.

### D. Discussion About the Torsional Oscillator

The exact values of mode function  $\theta(z)$  and resonance frequency  $\Omega$  depends on the detailed geometrical structure of the torsional resonator, here we use a method to estimate the rough profile of  $\theta(z)$ . Considering a suspended slender beam with two ends fixed, the corresponding wave equation for a cylinder with varying cross-section is known as Webster-type equation and takes the form [4]

$$c_t^{-2} \partial_t^2 \phi(t, z) - \partial_z^2 \phi(t, z) - \left( \frac{\partial_z I_p(z)}{I_p(z)} \right) \partial_z \phi(t, z) = 0 \quad (19)$$

where  $I_p(z) = \int_A r^2 dA$  is the polar moment of inertia at the cross section  $A(z)$  and  $c_t$  is the phase velocity of the torsional wave. To solve the wave equation, it is convenient to first separate it in time and space and construct solutions of the form  $\phi(t, z) = \theta(z) \cos(\Omega t)$ , so that only the differential equation in the axial coordinate remains.

In the simplest case where the torsional oscillator is a homogeneous cylinder, we have  $\partial_z I_p(z) = 0$ . Then the wave equation (19) will be reduced to its simplest form

$$\partial_z^2 \theta(z) + k_t^2 \theta(z) = 0, \quad (20)$$

with the well-known solutions:

$$\theta_s(z) = \sin(k_t z), \quad \theta_c(z) = \cos(k_t z), \quad \text{where } k_t = \Omega/c_t. \quad (21)$$

At the ends of the torsional oscillator,  $\theta(z) = 0$ , and we can derive the resonance frequency  $\Omega$  from the corresponding boundary condition. However, the torsional oscillator also includes other structures besides the square suspended beam and the mode function  $\theta(z)$  will be more complex than sine function or cosine function, and the effective moment of inertia  $I_{\text{eff}}$  will also larger than  $I_{\text{beam}} = 1/6 M a^2 \int_{-L/2}^{L/2} \theta(z)^2 dz = 1/12 \rho L a^4$ . As a simple example, we consider the fundamental mode of a suspended beam. The eigen wave vector  $k_t$  of the sine mode  $\sin(k_t z)$  is  $2\pi n/L$  with boundary condition  $\theta_s(L/2) = 0$ , where  $n$  is an integer, and the wave vector  $k_t$  of the cosine function mode  $\cos(k_t z)$  is  $2\pi(n + 1/2)/L$  with boundary condition  $\theta_c(L/2) = 0$ . Therefore, the fundamental mode function  $\theta(z)$  of the torsional oscillator should be an even function and the piece-wise mode function of the square beam should be a cosine function  $\cos(k_t z)$ . In our calculation, we assume  $\rho = 2650 \text{ kg/m}^3$ ,  $c_t = 5000 \text{ m/s}$  [5],  $L = 100 \mu\text{m}$ ,  $a = 1 \mu\text{m}$ ,  $\Omega = 2\pi \times 500 \text{ kHz}$ ,  $I_{\text{eff}} = 10 \times 1/6 \rho a^4 \int_{-L/2}^{L/2} \theta(z)^2 dz = 10/12 \rho L a^4 = 4.4163 \times 10^{-25} \text{ kg} \cdot \text{m}^2$  and  $k_t = \Omega/c_t = 100\pi/\text{m}$ . The parameters we will use is listed in Table (I).

Table I. Parameters used in calculation

$a/\mu\text{m}$	$L/\mu\text{m}$	$\rho/\text{kg} \cdot \text{m}^{-3}$	$\Omega/\text{kHz}$	$c_t/\text{km} \cdot \text{s}^{-1}$	$I_{\text{eff}}/\text{kg} \cdot \text{m}^2$	$k_t/\text{m}^{-1}$	$\beta_1/k$	$\beta_2/k$	$\epsilon_{xx}$	$\epsilon_{yy}$	$\epsilon_{zz}$
1	100	2650	$2\pi \times 500$	5.0	$4.4163 \times 10^{-25}$	$100\pi$	1.2859	1.2926	1.5326	1.5277	1.5277

### E. Calculation of the Coupling Constants

In this section we discuss the exact values of the coupling constants. When wavelength  $\lambda = 1550 \text{ nm}$ , the relative permittivity tensor of  $\alpha$ -quartz are [6]

$$\epsilon(0) = \begin{pmatrix} 1.5326^2 & 0 & 0 \\ 0 & 1.5277^2 & 0 \\ 0 & 0 & 1.5277^2 \end{pmatrix}, \quad (22)$$

and the corresponding mode profiles of the electric field  $\mathbf{E}_1$  and the electric field  $\mathbf{E}_2$  are plotted in Fig. (2).

*a.*  $g_{11MB} \approx 0$  and  $g_{22MB} \approx 0$  Because of the symmetry of the optical resonator,  $|\mathbf{E}_{i\parallel}(\mathbf{x})|^2$  and  $|\mathbf{D}_{i\perp}(\mathbf{x})|^2$  ( $i=x,y,z$ ) are even functions about  $x$  axis and  $y$  axis simultaneously. However, torsional mode function  $\mathbf{u}(\mathbf{x})$  is a odd function about  $x$  axis and  $y$  axis. Therefore, the integration  $g_{iMB}$  will approach 0.

*b.*  $g_{12MB} \approx 0$  Form Fig. (2) we know that  $\mathbf{E}_1(\mathbf{x})$  is a quasi- $x$  polarized electric field with  $|E_{1y}| \ll |E_{1x}|$  and  $\mathbf{E}_2(\mathbf{x})$  is a quasi- $y$  polarized electric field with  $|E_{2x}| \ll |E_{2y}|$ . In addition,  $\mathbf{E}_{1\parallel}(\mathbf{x})^\dagger \Delta \epsilon \mathbf{E}_{2\parallel}(\mathbf{x})$  usually can be expanded into the summation of  $E_{1m}(\mathbf{x})^\dagger \Delta \epsilon E_{2m}(\mathbf{x})$  ( $m = x, y, z$ ). Considering the normalized values of  $\mathbf{E}(\mathbf{x})$  and  $\mathbf{E}(\mathbf{x})$ ,

$$g_{12MB} \propto \sum_{m=x,y,z} \frac{\int (-E_{1m}^* \Delta \epsilon E_{2m} + D_{1m}^* \Delta(\epsilon^{-1}) D_{2m}) dA}{\sqrt{\int \mathbf{E}_1 \cdot \epsilon \mathbf{E}_1 dxdy} \cdot \sqrt{\int \mathbf{E}_2 \cdot \epsilon \mathbf{E}_2 dxdy}}, \quad (23)$$

Thus the value of  $g_{MB}$  will approach 0.

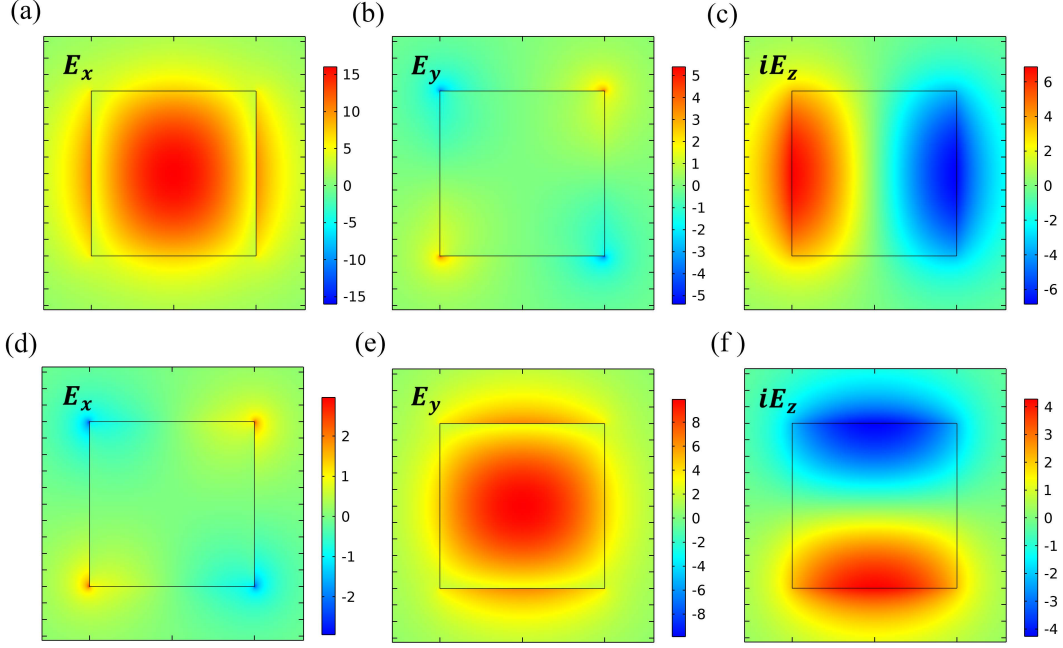


Figure 2. (a), (b) and (c) are the electric fields distribution of the TE-like mode. (d), (e) and (f) are the electric field distribution of the TM-like mode. It is obvious that  $|\mathbf{E}_i|^2$  ( $i=x,y,z$ ) is symmetric about  $x$  axis and  $y$  axis.

*c.*  $g_{ijOE} \approx 0$  The exact values of  $g_{ijOE}$  depends on the strain tensor  $s_{mn}$ , electric field  $\mathbf{E}_1(\mathbf{x})$  and electric field  $\mathbf{E}_2(\mathbf{x})$ . When the mode function  $\theta(z)$  of the torsional oscillator is a cosine function  $\theta(z) = \cos(k_t z)$ , the strain tensor  $s_{mn}$  is

$$\mathbf{s} = \frac{1}{2} \sin(k_t z) \frac{k_t}{R} \begin{pmatrix} 0 & 0 & y \\ 0 & 0 & -x \\ y & -x & 0 \end{pmatrix}. \quad (24)$$

In our main article, we assume that  $\mathbf{E}_i(\mathbf{x}) = \mathbf{E}_i(x, y) \cos(\beta_i z)$ . Substituting Equ. (24) into Equ. (18), we can easily derive the conclusion that

$$g_{ijOE} \propto \int_{-L/2}^{L/2} \sin(k_t z) \cos(\beta_i z) \cos(\beta_j z) dz = 0. \quad (25)$$

We need to note that we do not need the exact value of the Pockel's tensor  $p$ .

*d.*  $g_{11MA} \approx 0$  and  $g_{22MA} \approx 0$  The reason that  $g_{iiAM} \approx 0$  is similar with the reason that  $g_{12MB} = 0$ .

*e.*  $g_{12MA} \neq 0$  Considering the normalized condition of  $\mathbf{E}_1(\mathbf{x})$  and  $\mathbf{E}_2(\mathbf{x})$ , we can express  $g_{12MA}$  as

$$\begin{aligned} g_{12MA} &= \frac{\theta_{zp}}{2} \int_{V_1} dx dy (E_{1y}(x, y) E_{2x}^*(x, y) + E_{2y}^*(x, y) E_{1x}(x, y)) \times \int_{-L/2}^{L/2} \theta(z) \cos(\beta_1 z) \cos(\beta_2 z) dz \\ &= \frac{\theta_{zp}}{2} (\epsilon_{xx} - \epsilon_{yy}) \sqrt{\omega_1 \omega_2} \frac{\int (E_{2x} E_{1y}^* + E_{2y} E_{1x}^*) dx dy}{\sqrt{\int \mathbf{E}_1 \cdot \epsilon \mathbf{E}_1 dx dy} \cdot \sqrt{\int \mathbf{E}_2 \cdot \epsilon_2 \mathbf{E}_2 dx dy}} \times \frac{\int_{-L/2}^{L/2} \cos(k_t z) \cos(\beta_1 z) \cos(\beta_2 z) dz}{\sqrt{\int_{-L/2}^{L/2} \cos(\beta_1 z)^2 dz} \cdot \sqrt{\int_{-L/2}^{L/2} \cos(\beta_2 z)^2 dz}} \\ &\propto \theta_{zp} \sqrt{\omega_1 \omega_2} \left( \frac{\delta \epsilon}{L} \right) \int_{-L/2}^{L/2} \theta(z) \cos(\beta_1 z) \cos(\beta_2 z) dz. \end{aligned} \quad (26)$$

In the last step of Equ. (26), we use the approximation that  $\int_{-L/2}^{L/2} \cos(\beta_1 z)^2 dz \approx \int_{-L/2}^{L/2} \cos(\beta_2 z)^2 dz \approx L/2$ .



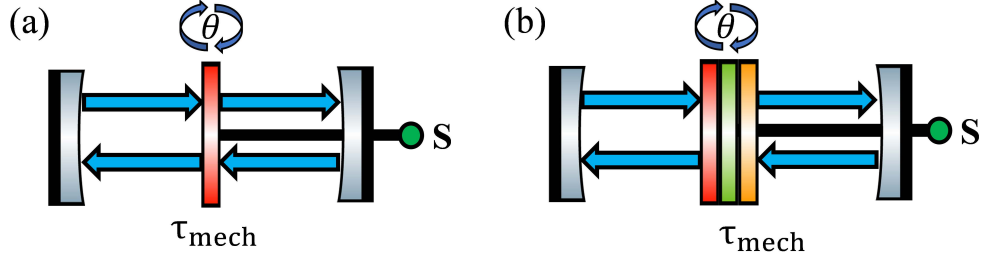


Figure 3. A simple example for our optomechanical model. (a) An extremely thin anisotropic membrane interacts with the cavity photons. Under the influencing the cavity photons, the membrane will experience a mechanical torque  $\tau_{\text{mech}}$ . (b) We stack several optical anisotropic dielectric membranes in this cavity. The total mechanical torque  $\tau_{\text{mech}}$  will be similar with the mechanical torque  $\tau_{\text{mech}}$  in (a).

*f. Discussion about  $g_{12AM}$*  If  $\theta(z) \propto \cos(k_t z)$ , then the expression of  $g_{12MA}$  will be

$$g_{12AM} \propto \frac{1}{L} \int_{-L/2}^{L/2} \cos(k_t z) \cos(\beta_1 z) \cos(\beta_2 z) dz$$

$$= -\frac{\sin(\frac{1}{2}L(-\beta_1 - \beta_2 + k_t))}{2L(\beta_1 + \beta_2 - k_t)} + \frac{\sin(\frac{1}{2}L(\beta_1 - \beta_2 + k_t))}{2L(\beta_1 - \beta_2 + k_t)} + \frac{\sin(\frac{1}{2}L(-\beta_1 + \beta_2 + k_t))}{2L(-\beta_1 + \beta_2 + k_t)} + \frac{\sin(\frac{1}{2}L(\beta_1 + \beta_2 + k_t))}{2L(\beta_1 + \beta_2 + k_t)}. \quad (27)$$

In this system,  $\beta_1 \sim 2\pi/\lambda$  and  $\beta_2 \sim 2\pi/\lambda$  where  $\lambda$  is the wavelength of the electromagnetic field. If  $L \geq 0.1\text{mm}$ ,  $\beta_1 L \gg 1$  and  $\beta_2 L \gg 1$ . When  $\beta_1 - \beta_2 = k_t \gg L^{-1}$ ,  $\frac{\sin(\frac{1}{2}L(\beta_1 - \beta_2 + k_t))}{(\beta_1 - \beta_2 + k_t)L} = \frac{\sin(k_t L)}{2k_t L} \ll 1$  and  $\frac{\sin(\frac{1}{2}L(\beta_1 - \beta_2 - k_t))}{2(\beta_1 - \beta_2 - k_t)L} = \frac{1}{4}$ . Notice that  $\theta_{zp} = \sqrt{\hbar/(2I_{\text{eff}}\Omega)} \propto L^{-1/2}$ , we have  $g \approx g_{12MA} \propto \delta\epsilon\theta_{zp} \propto \delta\epsilon L^{-1/2}$ .

Using the parameters listed in Table I, the exact values of  $g$  is listed in the following table:

Table II. Table about  $g$

$g_{12AM}/\text{kHz}$	$g_{11AM}/\text{kHz}$	$g_{22AM}/\text{kHz}$	$g_{12MB}/\text{kHz}$	$g_{11MB}/\text{kHz}$	$g_{22MB}/\text{kHz}$	$g_{iJOE}/\text{kHz}$
22	0	0	0.081	-0.01	-0.01	0

## F. A Simple Explanation For Our Optomechanical Hamiltonian

Considering the energy of the torsional oscillator and neglecting the optomechanical interaction terms  $a_1^\dagger a_1(b + b^\dagger)$  and  $a_2^\dagger a_2(b + b^\dagger)$ , the Hamiltonian of this system can be expressed as

$$H_{\text{OM}} = \hbar\Omega b^\dagger b + \hbar\omega_1 a_1^\dagger a_1 + \hbar\omega_2 a_2^\dagger a_2 + \hbar g(b + b^\dagger)a_1^\dagger a_2 + \hbar g^*(b + b^\dagger)a_2^\dagger a_1 \quad (28)$$

where  $g = g_{12MA} + g_{12OE} + g_{12MB} \approx g_{12AM}$ .

In order to understand this optomechanical interaction further, we consider a more physical and simpler example (see Fig. 3(a)): we use a laser beam with two orthogonal linear polarization modes  $a_x$  and  $a_y$  to interact with an optical anisotropic membrane with width  $d \ll \lambda$  and then calculate the optomechanical Hamiltonian. According to the angular momentum conservation law [7], along the direction of the optical axis  $z$ , the mechanical torque  $\tau_{\text{mech}}$  experienced by this membrane is

$$\tau_{\text{mech}} = -\tau_{\text{field}} - \left( \int_{\partial V} \overset{\leftrightarrow}{\mathbf{M}}(\mathbf{r}, t) \cdot \mathbf{n} dS \right)_z, \quad (29)$$

where  $\tau_{\text{field}} = \left( \frac{d}{dt} \frac{1}{c^2} \int_V \mathbf{r} \times (\mathbf{E} \times \mathbf{H}) dV \right)_z$  is the electromagnetic torque,  $\overset{\leftrightarrow}{\mathbf{M}}$  is optical angular momentum flux density and the integral  $\int_{\partial V} \overset{\leftrightarrow}{\mathbf{M}}(\mathbf{r}, t) \cdot \mathbf{n} dS$  is over the surface the membrane. In order to simple calculation, we define  $\mathcal{M}_{zz} = \left( \int_{\partial V} \overset{\leftrightarrow}{\mathbf{M}}(\mathbf{r}, t) \cdot \mathbf{n} dS \right)_z$ . Following the calculation, we can divide  $\mathcal{M}_{zz}$  into spin and orbit parts [8],

$$\mathcal{M}_{zz} = \mathcal{M}_{zz}^{\text{spin}} + \mathcal{M}_{zz}^{\text{orbit}} \quad (30)$$

where

$$\mathcal{M}_{zz}^{\text{spin}} = \frac{\epsilon_0 c^2}{2\omega} \text{Re} \left[ -i \iint \rho d\rho d\phi (\mathcal{E}_x \mathcal{B}_x^* + \mathcal{E}_y \mathcal{B}_y^*) \right] \quad (31)$$

and

$$\mathcal{M}_{zz}^{\text{orbit}} = \frac{\epsilon_0 c^2}{4\omega} \text{Re} \left[ -i \iint \rho d\rho d\theta (-\mathcal{B}_x^* \frac{\partial}{\partial \theta} \mathcal{E}_y + \mathcal{E}_y \frac{\partial}{\partial \theta} \mathcal{B}_x^* - \mathcal{E}_x \frac{\partial}{\partial \theta} \mathcal{B}_y^* + \mathcal{B}_y^* \frac{\partial}{\partial \theta} \mathcal{E}_x) \right]. \quad (32)$$

Under paraxial approximation, the corresponding E.M. fields are

$$\mathcal{E}_x = F_m(\rho) e^{im\theta} T_x(z) \hat{a}_x, \quad \mathcal{E}_y = F_m(\rho) e^{im\theta} T_y(z) \hat{a}_y, \quad (33)$$

$$\mathcal{B}_x = -\frac{F_m(\rho) e^{im\theta}}{i\omega} \frac{\partial T_y(z)}{\partial z} \hat{a}_y, \quad \mathcal{B}_y = \frac{F_m(\rho) e^{im\theta}}{i\omega} \frac{\partial T_x(z)}{\partial z} \hat{a}_x, \quad (34)$$

where  $m$  is quantum number of the orbital angular momentum,  $F_m(\rho)$  is the radial mode function and  $T_x(z)$ ,  $T_y(z)$  are the longitudinal mode functions. Without loss of generality, we assume that  $\iint d\rho d\phi |F(\rho)|^2 = 1$ . It is worth to notice that  $\mathcal{B}_x$  is related with operator  $\hat{a}_y$  and  $\mathcal{B}_y$  is related with operator  $\hat{a}_x$ . Using these equations, we can derive the operator of optical spin angular momentum flux  $\mathcal{M}_{zz}^{\text{spin}}$ :

$$\begin{aligned} \mathcal{M}_{zz}^{\text{spin}} &= \frac{\epsilon_0 c^2}{2\omega} \text{Re} \left[ -i \iint \rho d\rho d\theta (\mathcal{E}_x \mathcal{B}_x^* + \mathcal{E}_y \mathcal{B}_y^*) \right] \\ &= \frac{\epsilon_0 c^2}{4\omega^2} \left[ T_y(z) \frac{dT_x^*(z)}{dz} \hat{a}_x^\dagger \hat{a}_y - T_x(z) \frac{dT_y^*(z)}{dz} \hat{a}_y^\dagger \hat{a}_x \right] + h.c. \end{aligned} \quad (35)$$

Similarly, the optical orbital angular momentum flux  $\mathcal{M}_{zz}^{\text{orbit}}$  is

$$\begin{aligned} \mathcal{M}_{zz}^{\text{orbit}} &= m \frac{\epsilon_0 c^2}{2\omega} \text{Re} \left[ \iint \rho d\rho d\theta (-\mathcal{B}_x^* \mathcal{E}_y + \mathcal{E}_x \mathcal{B}_y^*) \right] \\ &= m \frac{\epsilon_0 c^2}{2\omega^2} \text{Re} \left[ i \frac{dT_y^*(z)}{dz} T_y(z) \right] \hat{a}_y^\dagger \hat{a}_y + m \frac{\epsilon_0 c^2}{2\omega^2} \text{Re} \left[ i \frac{dT_x^*(z)}{dz} T_x(z) \right] \hat{a}_x^\dagger \hat{a}_x. \end{aligned} \quad (36)$$

Notice that spin angular momentum flux  $\mathcal{M}_{zz}^{\text{spin}}$  involves the exchange interaction between two modes  $\hat{a}_x$  and  $\hat{a}_y$ , while orbital angular momentum flux  $\mathcal{M}_{zz}^{\text{orbit}}$  is proportional to photonic energy  $\hat{a}_x^\dagger \hat{a}_x$  and  $\hat{a}_y^\dagger \hat{a}_y$ . If the input beam does not carry orbital angular momentum, which means  $m = 0$ , we can easily prove that  $\mathcal{M}_{zz}^{\text{orbit}} = 0$  but  $\mathcal{M}_{zz}^{\text{spin}}$  is not influenced. If the input beam is a single frequency E.M. field, we can easily prove that  $\tau_{\text{field}} = 0$ . Then considering the condition  $d \ll \lambda$ , the mechanical torque  $\tau_z$  is

$$\iint dx dy (M_{zz}(x, y, 0^-) - M_{zz}(x, y, 0^+)) = \tau_{\text{mech}}. \quad (37)$$

Here we assume the dielectric membrane is in  $z = 0$ . The corresponding angular momentum optomechanical Hamiltonian is

$$H_{\text{OM}} = -\hat{\tau}_{\text{mech}} \hat{\theta} = -\hat{\tau}_{\text{mech}}^{\text{spin}} \hat{\theta} - \hat{\tau}_{\text{mech}}^{\text{orbit}} \hat{\theta} = H_{\text{OM}}^{\text{Spin}} + H_{\text{OM}}^{\text{Orbit}}, \quad (38)$$

where  $H_{\text{OM}}^{\text{Spin}} = -\hat{\tau}_{\text{mech}}^{\text{spin}} \hat{\theta}$  and  $H_{\text{OM}}^{\text{Orbit}} = -\hat{\tau}_{\text{mech}}^{\text{orbit}} \hat{\theta}$ . Considering Equ.(35) and Equ.(36), we know that

$$H_{\text{OM}}^{\text{Spin}} \propto (g_{\text{spin}} \hat{a}_x^\dagger \hat{a}_y + g_{\text{spin}}^* \hat{a}_y^\dagger \hat{a}_x) \hat{\theta}, \quad H_{\text{OM}}^{\text{Orbit}} \propto m(g_x \hat{a}_x^\dagger \hat{a}_x + g_y \hat{a}_y^\dagger \hat{a}_y) \hat{\theta}. \quad (39)$$

Essentially, our optomechanical system can be viewed as the stacking of several optical anisotropic dielectric membranes (Fig. 3(b)). Therefore, the optomechanical Hamiltonian of our system also has the form  $H_{\text{OM}} \propto (ga_x^\dagger a_y + h.c.) \hat{\theta} = (ga_x^\dagger a_y + h.c.) (b + b^\dagger)$ .

## II. DISCUSSION ABOUT INPUT-OUTPUT RELATION

### A. Mechanical Mode

When the mechanical frequency  $\Omega$  is much smaller than the optical pulse bandwidth,  $\Omega \ll \tau^{-1}$ , the mechanical oscillator Hamiltonian  $H_M = \hbar \Omega b^\dagger b$  and mechanical damping characterized by the mechanical damping rate  $\gamma = \Omega/Q_t$  can be neglect in the time scale of a single optical pulse.

### B. Optical Mode $a_2$

If we use the original form of  $H_{OM}$  (28), we can derive the Langevin equation of the optical mode  $a_2$ ,

$$\dot{a}_2 = -\frac{\kappa}{2}a_2 - \sqrt{2}g\theta_M a_1 + \sqrt{\kappa}a_{2in}(t) \quad (40)$$

where  $\kappa$  is the decaying rate of the cavity. If the input mode  $a_{2in}(t)$  is a intense coherent laser pulse with duration  $\tau$ , we can neglect weak coupling term  $\sqrt{2}g\theta_M a_1$ . In our following discussion, we only consider the classical amplitude of mode  $a_2$  and we define that  $\langle a_2 \rangle = \alpha_2$ . When  $\kappa \gg \tau^{-1}$ , we can eliminate the dynamics of the intra-cavity field  $a_2$  adiabatically, yielding a simple relation between the external and internal field amplitudes:

$$\frac{d\alpha_2(t)}{dt} \approx -\frac{\kappa}{2}\alpha_2(t) + \sqrt{\kappa}\alpha_{2in}(t) \approx 0 \Rightarrow \alpha_2(t) = \frac{2}{\sqrt{\kappa}}\alpha_{2in}(t). \quad (41)$$

We assume the temporal function of  $a_{2in}(t)$  is  $f(t)$  with an envelop of duration  $\tau$ .  $f(t)$  satisfies the normalized condition  $\int_{-\infty}^{\infty} f(t)^2 dt = 1$ . If the photon number of a single pulse is  $N_{in}$ , then  $\alpha_{2in}$  becomes  $\alpha_{2in}(t) = \sqrt{N_{in}}f(t)$ . It is easy to verify that  $\int_{-\infty}^{\infty} |\alpha_{2in}(t)|^2 dt = N_{in}$ , which shows the photon number of single pulse is  $N_{in}$ . At this case,  $\alpha_2(t)$  can be expressed as

$$\alpha_2(t) = \frac{2}{\sqrt{\kappa}}\alpha_{2in}(t) = 2\sqrt{\frac{N_{in}}{\kappa}}f(t) = \alpha f(t), \quad (42)$$

where  $\alpha = 2\sqrt{\frac{N_{in}}{\kappa}}$  is the amplitude of  $\alpha_2(t)$ .

### C. Input-Output Relation

Neglecting phonon energy  $H_m = \hbar\Omega b^\dagger b$  and using  $\alpha_2(t)$  to replace operator  $a_2$ , we can describe the dynamics of the optical and mechanical quadrature operators by the set of the following Langevin equations:

$$\begin{aligned} \frac{dx_L(t)}{dt} &= -\frac{\kappa}{2}x_L(t) + \sqrt{\kappa}x_L^{\text{in}}(t), \\ \frac{dp_L(t)}{dt} &= -2g\alpha_2(t)\theta_M - \frac{\kappa}{2}p_L(t) + \sqrt{\kappa}p_L^{\text{in}}(t), \\ \frac{d\theta_M}{dt} &= 0, \\ \frac{dL_M}{dt} &= -2g\alpha_2(t)x_L(t) \end{aligned} \quad (43)$$

where  $x_L^{\text{in}}(t)$  and  $p_L^{\text{in}}(t)$  are the quadratures of input noise, which satisfy the commutation relation  $[x_L^{\text{in}}(t), p_L^{\text{in}}(t')] = i\delta(t - t')$ . Invoking adiabatic elimination of the optical intra-cavity field  $\frac{dx_L(t)}{dt} \approx 0$  and  $\frac{dp_L(t)}{dt} \approx 0$ , we will have the following equations

$$x_L(t) = \frac{2}{\sqrt{\kappa}}x_L^{\text{in}}(t), \quad p_L(t) = \frac{2}{\sqrt{\kappa}}p_L^{\text{in}}(t) - \frac{4g\alpha_2(t)}{\kappa}\theta_M. \quad (44)$$

By means of the usually optical input-output relation  $a_1^{\text{out}}(t) + a_1^{\text{in}}(t) = \sqrt{\kappa}a_1(t)$  we find:

$$\begin{aligned} x_L^{\text{out}}(t) &= x_L^{\text{in}}(t), \\ p_L^{\text{out}}(t) &= p_L^{\text{in}}(t) - \frac{4g\alpha_2(t)}{\sqrt{\kappa}}\theta_M(t), \\ \frac{d\theta_M}{dt} &= 0, \\ \frac{dL_M}{dt} &= -2g\alpha_2(t)x_L(t), \end{aligned} \quad (45)$$

In order to derive the inout-output in our main article, we define time collective optical quadratures  $x_L^{\text{in/out}} = \int_{-\infty}^{\infty} f(t)x_L^{\text{in/out}}(t)dt$ ,  $p_L^{\text{in/out}} = \int_{-\infty}^{\infty} f(t)p_L^{\text{in/out}}(t)dt$ . It is easy to verify that  $x_L^{\text{in/out}}$  and  $p_L^{\text{in/out}}$  also satisfy the standard commutation  $[x_L^{\text{in/out}}, p_L^{\text{in/out}}] = i$ .

Besides, we define  $\theta_M^{\text{in}} = \theta_M(t = -\infty)$  and  $\theta_M^{\text{out}} = \theta_M(t = +\infty)$ . As  $\alpha_2(t)$  is a short pulse,  $\theta_M^{\text{in}}$  and  $\theta_M^{\text{out}}$  represent the  $\theta_M$  quadrature before and after the optomechanical interaction, respectively.

Firstly, from equation  $\frac{d\theta_M}{dt} = 0$  we know that  $\theta_M(t) = \theta_M^{\text{in}} = \theta_M^{\text{out}}$ , which means that  $\theta_M(t)$  is a constant operator during the optomechanical interaction. Secondly, multiplying the equation  $x_L^{\text{out}}(t) = x_L^{\text{in}}(t)$  by  $f(t)$  and integrating it over the whole time interval, we will obtain the equation  $x_L^{\text{out}} = x_L^{\text{in}}$ . Similarly, also multiplying the equation  $p_L^{\text{out}}(t) = p_L^{\text{in}}(t) - \frac{4g\alpha_2(t)}{\sqrt{\kappa}}\theta_M$  by  $f(t)$  and integrating it over the whole time interval, we will have  $p_L^{\text{out}} = p_L^{\text{in}} - \frac{4g}{\sqrt{\kappa}} \int_{-\infty}^{\infty} f(t)\alpha_2(t)\theta_M(t)dt = p_L^{\text{in}} - \frac{4g\theta_M^{\text{in}}}{\sqrt{\kappa}} \int_{-\infty}^{\infty} f(t)\alpha_2(t)dt$ .

Defining  $\chi = \frac{4g}{\sqrt{\kappa}} \int_{-\infty}^{\infty} f(t)\alpha_2(t)dt$ , and considering Equ. (42)  $\alpha_2(t) = \alpha f(t)$ , we have

$$\chi = \frac{4g}{\sqrt{\kappa}} \int_{-\infty}^{\infty} f(t)\alpha_2(t)dt = \frac{4g}{\sqrt{\kappa}} \int_{-\infty}^{\infty} \alpha f(t)^2 dt = \frac{4g\alpha}{\sqrt{\kappa}} = \frac{8g\sqrt{N_{\text{in}}}}{\kappa} = \frac{4g}{\sqrt{\kappa}} \sqrt{\int_{-\infty}^{\infty} |\alpha_2(t)|^2 dt}. \quad (46)$$

As a consequence, we have  $p_L^{\text{out}} = p_L^{\text{in}} - \chi\theta_M^{\text{in}}$ . Thirdly, from equation  $\frac{dL_M}{dt} = -2g\alpha_2(t)x_L(t)$  we know that  $L_M^{\text{out}} - L_M^{\text{in}} = -2g \int_{-\infty}^{\infty} \alpha_2(t)x_L(t)dt$ . Using Equ. (44)  $x_L(t) = \frac{2}{\sqrt{\kappa}}x_L^{\text{in}}(t)$ , we will derive the equation  $L_M^{\text{out}} - L_M^{\text{in}} = -4g/\sqrt{\kappa} \int_{-\infty}^{\infty} \alpha_2(t)x_L^{\text{in}}(t)dt = -\frac{4g\alpha}{\sqrt{\kappa}}x_L^{\text{in}} = -\chi x_L^{\text{in}}$ .

Finally, we will derive this set of input-output relation

$$\begin{aligned} x_L^{\text{out}} &= x_L^{\text{in}}, \\ p_L^{\text{out}} &= p_L^{\text{in}} - \chi\theta_M^{\text{in}}, \\ \theta_M^{\text{out}} &= \theta_M^{\text{in}}, \\ L_M^{\text{out}} &= L_M^{\text{in}} - \chi x_L^{\text{in}}. \end{aligned} \quad (47)$$

### III. WIGNER FUNCTION FORMALISM

For a continuous variable quantum system, if the initial states, the system evolution and the measurement process are all Gaussian, the whole system can advantageously be modeled using standard Gaussian formalism. However, in our system, the input optical state is non-Gaussian state and we must use other method to derive the Wigner function of the resulting mechanical state.

#### A. General Definition of Wigner function

For a  $n$  modes Bosonic system, the Wigner function is defined by

$$W(\mathbf{r}) = \frac{1}{(2\pi)^{2n}} \int d^{2n}\boldsymbol{\beta} \text{Tr}\{\hat{\rho}\hat{D}(\boldsymbol{\beta})\} \exp\{-i\mathbf{r}^T \cdot \Omega\boldsymbol{\beta}\}, \quad (48)$$

in which the  $2n \times 2n$  matrix  $\Omega$  is the  $n$ -fold block diagonal matrix with diagonal blocks  $\varpi = \begin{pmatrix} 0 & 1 \\ -1 & 0 \end{pmatrix}$  and  $\hat{D}(\boldsymbol{\beta})$  is the multi-mode displacement operator with  $\boldsymbol{\beta}^T = (\Re\{\beta_1\}, \Im\{\beta_1\}, \Re\{\beta_2\}, \dots)$  giving the displacement of each mode. Points in phase space are denoted  $\mathbf{r}^T = (x_1, p_1, x_2, \dots)$  and  $\mathbf{r} \cdot \Omega\boldsymbol{\beta} = \sum_{i=1}^n (-p_i\Re\{\beta_i\} + x_i\Im\{\beta_i\})$ . For a single mode state, displacement operator  $\hat{D}(\beta)$  is defined as  $\hat{D}(\beta) = \exp(\beta a^\dagger - \beta a)$ . If we define  $\hat{x} = a^\dagger + a$ ,  $\hat{p} = i(a^\dagger - a)$ , and  $\hat{\mathbf{r}} = (\hat{x}, \hat{p})$ , then  $\beta a^\dagger - \beta a = i(\Im\{\beta\}\hat{x} - \Re\{\beta\}\hat{p}) = i\hat{\mathbf{r}}^T \cdot \Omega\boldsymbol{\beta}$ . Therefore, displacement operator can also be expressed as  $\hat{D}(\boldsymbol{\beta}) = \exp(i\hat{\mathbf{r}} \cdot \Omega\boldsymbol{\beta})$ . The Wigner function is Fourier dual to the characteristic function  $\chi(\boldsymbol{\beta}) = \text{Tr}\{\hat{\rho}\hat{D}(\boldsymbol{\beta})\}$ ,

$$\chi(\boldsymbol{\beta}) = \int d^{2n}\mathbf{r} W(\mathbf{r}) \exp\{+i\mathbf{r}^T \cdot \Omega\boldsymbol{\beta}\} \quad (49)$$

and it is easy to verify that  $\chi(0) = \text{Tr}[\hat{\rho}] = 1$ .

### B. Time evolution of Wigner function

If the time evolution of all the quadratures  $\hat{r}$  of a bosonic system can be described by a linear transformation, which means that

$$\hat{r}(T) = M\hat{r}(0), \quad (50)$$

then the Wigner function and characteristic function of this system at time  $T$  can also be totally described by matrix  $M$  and the original density matrix  $\hat{\rho}(0)$ . In order to connect the Wigner function  $W(\mathbf{r}, T)$  of this system at time  $T$  with the Wigner function  $W(\mathbf{r}, 0)$ , we consider the following calculation. Firstly, we consider the time evolution of characteristic function. At time  $T$ , the displacement operator is

$$\hat{D}(\boldsymbol{\beta}, T) = \exp[i\hat{\mathbf{r}}(T)^T \cdot \Omega\boldsymbol{\beta}] = \exp[i(M\hat{\mathbf{r}}(0))^T \cdot \Omega\boldsymbol{\beta}] = \exp[i\boldsymbol{\beta}^T \Omega^T M\hat{\mathbf{r}}(0)]. \quad (51)$$

If we define a vector  $\boldsymbol{\gamma} = \Omega M^T \Omega \boldsymbol{\beta}$ , then we will have the following relation

$$\begin{aligned} \boldsymbol{\beta}^T \Omega^T M\hat{\mathbf{r}}(0) &= -\boldsymbol{\beta}^T \Omega^T M \Omega \Omega^T \hat{\mathbf{r}}(0) \\ &= \boldsymbol{\beta}^T (-\Omega^T M \Omega) \Omega^T \hat{\mathbf{r}}(0) \\ &= \boldsymbol{\beta}^T (\Omega M \Omega) \Omega^T \hat{\mathbf{r}}(0) \\ &= \boldsymbol{\gamma}^T \Omega^T \hat{\mathbf{r}}(0) \\ &= \hat{\mathbf{r}}(0)^T \cdot \Omega \boldsymbol{\gamma}. \end{aligned} \quad (52)$$

Therefore, at time  $T$

$$\hat{D}(\boldsymbol{\beta}, T) = \exp[\hat{\mathbf{r}}(0)^T \cdot \Omega \boldsymbol{\gamma}] = \hat{D}(\boldsymbol{\gamma}, 0). \quad (53)$$

The corresponding characteristic is

$$\chi(\boldsymbol{\beta}, T) = \text{Tr}[\hat{\rho}(T)\hat{D}(\boldsymbol{\beta}, 0)] = \text{Tr}[\hat{\rho}(0)\hat{D}(\boldsymbol{\beta}, T)] = \chi(\boldsymbol{\gamma}, 0). \quad (54)$$

Secondly, we consider the time evolution of Wigner function. If we define  $\Omega M^T \Omega = K$ , then  $\boldsymbol{\gamma} = K\boldsymbol{\beta}$ . At time  $T$ ,

$$W(\mathbf{r}, T) = \frac{1}{(2\pi)^{2n}} \int d^{2n}\boldsymbol{\beta} \chi(\boldsymbol{\beta}, T) \exp\{-i\mathbf{r}^T \cdot \Omega\boldsymbol{\beta}\} = \frac{1}{(2\pi)^{2n}} \int d^{2n}\boldsymbol{\beta} \chi(K\boldsymbol{\beta}, 0) \exp\{-i\mathbf{r}^T \cdot \Omega\boldsymbol{\beta}\}. \quad (55)$$

Using coordination transformation  $\boldsymbol{\beta}' = K\boldsymbol{\beta}$ , then

$$\mathbf{r}^T \cdot \Omega\boldsymbol{\beta} = \mathbf{r}^T \cdot \Omega K^{-1}\boldsymbol{\beta}' = \mathbf{r}^T \cdot (M^{-1})^T \Omega^{-1}\boldsymbol{\beta}' = (M^{-1}\mathbf{r})^T \cdot \Omega\boldsymbol{\beta}'. \quad (56)$$

Therefore, the Wigner function of the total system at time  $T$  is

$$W(\mathbf{r}, T) \propto \frac{1}{(2\pi)^{2n}} \int d^{2n}\boldsymbol{\beta}' \chi(\boldsymbol{\beta}', 0) \exp\{-i(M^{-1}\mathbf{r})^T \cdot \Omega\boldsymbol{\beta}'\} = W(M^{-1}\mathbf{r}, 0). \quad (57)$$

Here we use " $\propto$ " instead of " $=$ " is that we do not calculate the Jacobin matrix during the process of coordination transformation  $\boldsymbol{\beta}' = K\boldsymbol{\beta}$ .

### C. The Resulting Wigner Function

For our optomechanical system, if we neglect all of the noises and only care about the torsional mode  $b$  and optical mode  $a_1$ , the transformation matrix  $M$  is

$$M = \begin{pmatrix} 1 & 0 & 0 & 0 \\ 0 & 1 & -\chi & 0 \\ 0 & 0 & 1 & 0 \\ -\chi & 0 & 0 & 1 \end{pmatrix}, \quad (58)$$

which is derived from the input-output relation (47).



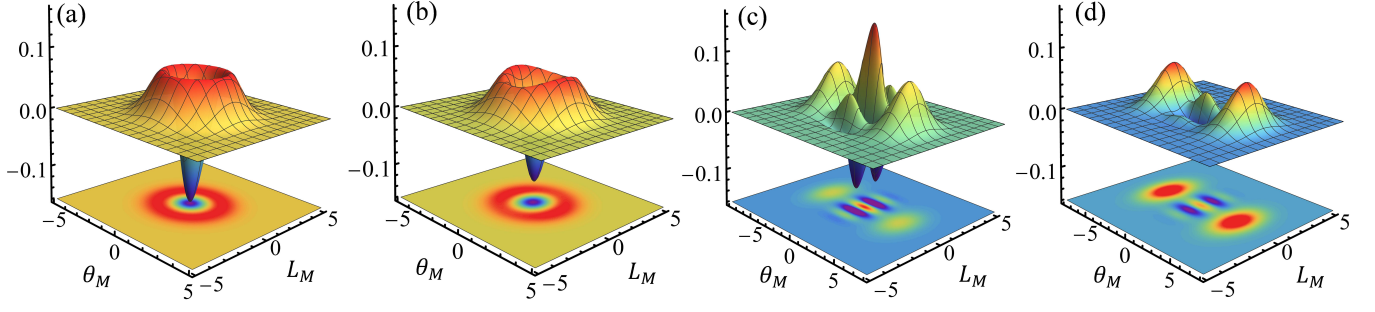


Figure 4. (a) Wigner Function of single phonon fock state. (b) Wigner function  $W_{\text{sfoc}}(\theta_M, L_M)$ . Here we set  $V_{LL} = 2000$  and  $V_{\theta\theta} = 0.2$ . (c) Wigner function of cat state with  $\alpha = 2$ . (d) Wigner function  $W_{\text{scat}}(\theta_M, L_M)$ . Here we also set  $V_{LL} = 2000$  and  $V_{\theta\theta} = 0.2$ .

We assume the initial quantum state  $\rho(0) = \rho_L \otimes \rho_M$ , where  $\rho_L$  is the density matrix of the input optical mode  $a_{\text{lin}}$  and  $\rho_M$  is the density matrix of the mechanical mode. The initial Wigner function is  $W(\mathbf{r}, 0) = W_L(x_L, p_L)W_M(x_M, p_M)$ . After the optomechanical interaction (47), the Wigner function of this system is

$$W(\mathbf{r}, T) = W(M^{-1}\mathbf{r}, 0) = W_L(x_L, p_L + \chi x_M)W_M(x_M, p_M + \chi x_L). \quad (59)$$

If we do a quantum measurement on the subsystem  $\rho_L$  with POVM measurement operator  $\Pi$ , then the resulting Wigner function is

$$W_{\text{meas}}(x_M, p_M) \propto \int d^2\mathbf{r}_L W(\mathbf{r}) W_{\Pi}(x_L, p_L), \quad (60)$$

where

$$W_{\Pi}(\mathbf{r}) = \frac{1}{(2\pi)^{2n}} \int d^{2n}\beta \text{Tr}\{\Pi \hat{D}(\beta)\} \exp\{-i\mathbf{r}^T \cdot \Omega\beta\}, \quad (61)$$

which is the Wigner function of the measurement operator  $\Pi$ . In the field of quantum optics, the most commonly used measurements are photon number detection, homodyne detection and heterodyne detection.

*a. Photon Number Detection* The POVM operator for photon number resolved detection with detection efficiency  $\eta$  is  $\Pi = \Pi_m(\eta) = \eta^m \sum_{k=m}^{\infty} (1-\eta)^{k-m} C_m^k |k\rangle\langle k|$  where  $C_m^k = \frac{m!}{k!(m-k)!}$ . The corresponding Wigner function [9]

$$W(X, Y) = \frac{1}{2\pi} \frac{(-1)^m \eta^m}{(2-\eta)^{1+m}} L_m \left( \frac{(X^2 + Y^2)}{2-\eta} \right) \exp \left\{ -\frac{\eta}{2(2-\eta)} (X^2 + Y^2) \right\} \quad (62)$$

where  $L_k(x)$  is a Laguerre polynomials.

*b. Homodyne Detection* If we use a photodetector with efficiency  $\eta = 1$  to detect the quadrature operator  $X_\phi = ae^{-i\phi} + a^\dagger e^{i\phi}$  with the measurement result  $x$ , then the corresponding POVM is  $\Pi(x) = |x\rangle_\phi \langle x|$ , where  $X_\phi |x\rangle_\phi = x |x\rangle_\phi$  and the corresponding Wigner functions is given [9]

$$W(X, P) \propto \delta(x - X \cos(\phi) - Y \sin(\phi)). \quad (63)$$

In our article, after the ideal homodyne detection of the output optical mode, the Wigner function of the resulting mechanical state is

$$W_{\text{meas}}(\theta_M, L_M) \propto \int d^2\mathbf{r}_L W_L(x_L, p_L + \chi\theta_M) W_M(\theta_M, L_M + \chi x_L) \delta(p_L - p) \quad (64)$$

where  $p$  is the result of the homodyne detection and in our numerical calculation we will choose  $p = 0$ .

*c. Single Photon Pulse Input* Here we consider a special and simple example: the original input optical state is a single photon fock state pulse with Wigner function  $W_L(x, p) \propto \exp(-\frac{1}{2}x^2 - \frac{1}{2}p^2)(x^2 + p^2 - 1)$  and the original mechanical state is a precooled thermal squeezed state  $W_M(\theta_M, L_M) \propto \exp\left[-\frac{\theta_M^2}{2V_{\theta\theta}} - \frac{L_M^2}{2V_{LL}}\right]$  where  $V_{LL}$  and  $V_{\theta\theta}$  are the variance of  $L_M$  and  $\theta_M$ , respectively. When  $p = 0$ , the resulting mechanical state is

$$W_{\text{sfoc}}(\theta_M, L_M) \propto \exp\left[-\frac{1}{2}(1 + V_{LL}^{-1})\theta_M^2 - \frac{1}{2}(1 + V_{\theta\theta}^{-1})L_M^2\right] [(1 + V_{\theta\theta})\theta_M^2 + (1 + V_{\theta\theta})^{-1}L_M^2 - 1]. \quad (65)$$

If  $V_{LL} \gg 1$ , Wigner function  $W_{\text{sfoc}}(\theta_M, L_M)$  will near the Wigner function of squeezed single phonon fock state and when  $V_{LL} \rightarrow \infty$  and  $V_{\theta\theta} \rightarrow 0$ ,  $W_{\text{meas}}(\theta_M, L_M)$  will near the Wigner function of single phonon fock state (see Fig. 4).

*d. Perfect Cat State Input* Now we consider a more complex case: the input optical state is a perfect even cat state  $|Cat\rangle \propto |\alpha\rangle + |-\alpha\rangle$ . Without loss of generality, we assume that  $\alpha$  is positive real value. For this even cat state, the corresponding Wigner function is

$$W_\alpha(\mathbf{r}) = \frac{e^{-\frac{1}{2}\mathbf{r} \cdot \mathbf{r}}}{2\pi(1 + e^{-2|\alpha|^2})} \left[ e^{-2|\alpha|^2} \cosh(2\mathbf{r} \cdot \boldsymbol{\alpha}) + \cos(2\mathbf{r} \cdot \boldsymbol{\varpi}\boldsymbol{\alpha}) \right], \quad (66)$$

where  $\mathbf{r} = (x_L, p_L)$  and  $\boldsymbol{\varpi} = \begin{pmatrix} 0 & 1 \\ -1 & 0 \end{pmatrix}$ . As for the mechanical state  $W_M(\theta_M, L_M)$ , we also assume that it is a thermal squeezed state. Assuming the homodyne result  $p = 0$ , the Wigner function of the resulting mechanical state is

$$W_{\text{scat}}(\theta_M, L_M) \propto \exp \left[ -\frac{1}{2}(1 + V_{LL}^{-1})\theta_M^2 - \frac{1}{2}(1 + V_{\theta\theta})^{-1}L_M^2 \right] \left[ \cos\left(\frac{2\alpha}{1 + V_{\theta\theta}}L_M\right) + \exp\left(-\frac{2\alpha^2}{1 + V_{\theta\theta}}\right) \cosh(2\alpha\theta_M) \right]. \quad (67)$$

Notice that when  $V_{LL} \rightarrow \infty$  and  $V_{\theta\theta} \rightarrow 0$ ,  $W_{\text{scat}}(\theta_M, L_M)$  will near the Wigner function of cat state (see Fig. 4).

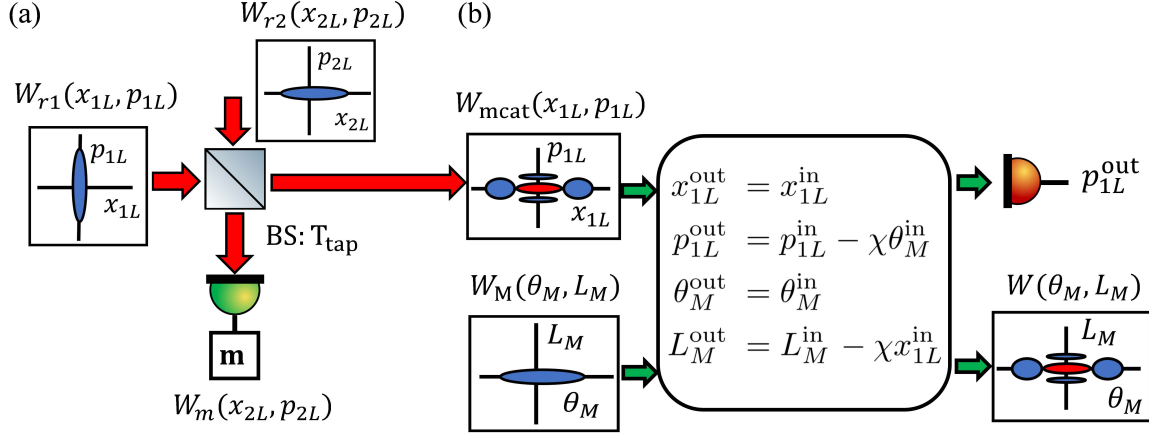


Figure 5. (a) The preparing process of the optical cat state with Wigner function  $W_{\text{mcat}}(x_{1L}, p_{1L})$ . BS is a beam splitter with transmittance  $T_{\text{tap}}$ ,  $m$  represents the photon number resolving detection with  $m$  photons detected and  $W_m(x_{2L}, p_{2L})$  is the corresponding Wigner function. (b) State transformation and preparing process of the resulting mechanical cat-like state with Wigner function  $W(\theta_M, L_M)$ . The input mechanical state  $W_M(\theta_M, L_M)$  is a squeezed thermal state along  $\hat{L}_M$  quadrature and  $p_{1L}^{\text{out}}$  represents the homodyne detection on the output optical quadrature  $\hat{p}_{1L}^{\text{out}}$ .

*e. Catlike State Prepared by Generalized Photon Subtracted Method* Following the calculation in ref [10], we discuss the Wigner function of the catlike state prepared by generalized photon subtracted method (see Fig. 5). For a squeezed state with squeezing parameter  $r$  ( $r$  is real number), the corresponding Wigner function  $W_r(x_L, p_L)$  is

$$W_r(x_L, p_L) \propto \exp \left[ -\frac{x_L^2}{2\exp(2r)} - \frac{p_L^2}{2\exp(-2r)} \right]. \quad (68)$$

In the generalized photon subtracted method, the original optical input state are two unentangled squeezed with squeezing parameter  $r_1$  and  $r_2$ . The corresponding Wigner function of the input state is

$$W_{\text{Lin}}(x_{1L}, p_{1L}, x_{2L}, p_{2L}) \propto W_{r_1}(x_{1L}, p_{1L})W_{r_2}(x_{2L}, p_{2L}). \quad (69)$$

The asymmetric beam splitter with transmittance  $T_{\text{tap}}$  exchanges the quantum state of the two squeezed light. If we define  $\hat{\mathbf{r}}_L = (\hat{x}_{1L}, \hat{p}_{1L}, \hat{x}_{2L}, \hat{p}_{2L})$ , then after the interaction of the beam splitter, the resulting optical quadratures will be

$$\hat{\mathbf{r}}_L \rightarrow M_L \hat{\mathbf{r}}_L, \quad (70)$$

where  $M_L$  is the transmission matrix of the beam splitter, and the exact form of  $M_L$  is

$$M_L = \begin{pmatrix} \sqrt{T_{\text{tap}}} & 0 & \sqrt{1-T_{\text{tap}}} & 0 \\ 0 & \sqrt{T_{\text{tap}}} & 0 & \sqrt{1-T_{\text{tap}}} \\ -\sqrt{1-T_{\text{tap}}} & 0 & \sqrt{T_{\text{tap}}} & 0 \\ 0 & -\sqrt{1-T_{\text{tap}}} & 0 & \sqrt{T_{\text{tap}}} \end{pmatrix}. \quad (71)$$

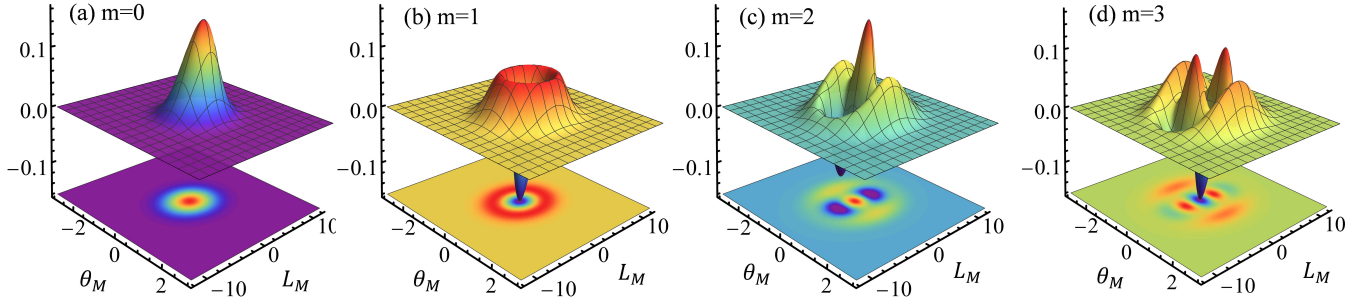


Figure 6. Wigner functions of optical catlike state prepared by generalized photon subtraction method. In numerical calculation, we choose  $r_1 = -r_2 = 1.15$  and  $T_{\text{tap}} = (e^{2r_1} - 1)/(e^{2r_1} - e^{-2r_1}) \approx 0.909$ . Here  $m$  represents the detected photon number.

According to the time evolution formalism of Wigner function (57), after the beam splitter, the corresponding optical Wigner function  $W_{L_{\text{tap}}}$  is

$$W_{L_{\text{tap}}}(x_{1L}, p_{1L}, x_{2L}, p_{2L}) \propto W_{\text{Lin}}(M_L^{-1}r_L). \quad (72)$$

Then we will do photon number resolved detection on the output port of squeezed light  $r_2$ . The corresponding measurement Wigner function  $W_m(x_{L2}, p_{L2})$  is Equ. (62), notice that  $W_m(x_{L2}, p_{L2})$  depends on the detected photon number  $m$ . Following the photon number resolved detection, the photon on the other port will be projected into a catlike state, and the exact expression of the resulting Wigner function is

$$W_{\text{mcat}}(x_{1L}, p_{1L}) \propto \int dx_{2L} dp_{2L} W_{L_{\text{tap}}}(x_{1L}, p_{1L}, x_{2L}, p_{2L}) W_m(x_{L2}, p_{L2}). \quad (73)$$

Following these processes, we prepare a optical catlike state. The Wigner function of the prepared optical catlike states are plotted in Fig. (6). When  $m > 1$ , the resulting Wigner function shows the feature of catlike state.

By using this optical catlike state pulse to pump the optical mode  $a_1$  in our optomechanical system, we can prepare our torsional oscillator in a catlike state, and the Wigner function of the resulting mechanical state is

$$W(\theta_M, L_M) \propto \int d^2x_{1L} dp_{1L} W_{\text{mcat}}(x_{1L}, p_{1L} + \chi\theta_M) W_M(\theta_M, L_M + \chi x_L) \delta(p_{1L} - p). \quad (74)$$

For different detected photon number  $m$ ,  $W_{\text{mcat}}$  will be different, thus  $W(\theta_M, L_M)$  will also be different.

- 
- [1] Steven G. Johnson, M. Ibanescu, M. A. Skorobogatiy, O. Weisberg, J. D. Joannopoulos, and Y. Fink. Perturbation theory for maxwell's equations with shifting material boundaries. *Phys. Rev. E*, 65:066611, Jun 2002.
  - [2] Hashem Zoubi and Klemens Hammerer. Optomechanical multimode hamiltonian for nanophotonic waveguides. *Phys. Rev. A*, 94:053827, Nov 2016.
  - [3] D. F. Nelson and M. Lax. Theory of the photoelastic interaction. *Phys. Rev. B*, 3:2778–2794, Apr 1971.
  - [4] C. Wuttke, G. D. Cole, and A. Rauschenbeutel. Optically active mechanical modes of tapered optical fibers. *Phys. Rev. A*, 88:061801, Dec 2013.
  - [5] Robert O. Pohl, Xiao Liu, and EunJoo Thompson. Low-temperature thermal conductivity and acoustic attenuation in amorphous solids. *Rev. Mod. Phys.*, 74:991–1013, Oct 2002.
  - [6] Gorachand Ghosh. Dispersion-equation coefficients for the refractive index and birefringence of calcite and quartz crystals. *Optics Communications*, 163(1):95–102, 1999.
  - [7] Lukas Novotny and Bert Hecht. *Principles of nano-optics*. Cambridge university press, 2012.
  - [8] Stephen M Barnett. Optical angular-momentum flux. *Journal of Optics B: Quantum and Semiclassical Optics*, 4(2):S7–S16, jan 2002.
  - [9] Alessandro Ferraro, Stefano Olivares, and Matteo G. A. Paris. Gaussian states in continuous variable quantum information. 2005.
  - [10] Kan Takase, Jun-ichi Yoshikawa, Warit Asavanant, Mamoru Endo, and Akira Furusawa. Generation of optical schrödinger cat states by generalized photon subtraction. *Phys. Rev. A*, 103:013710, Jan 2021.